Journal of Paleontology, 87(6), 2013, p. 1077–1106

0022-3360/13/0087-1077$03.00
DOI: 10.1666/12-121

REVISION AND EVALUATION OF THE SYSTEMATIC AFFINITY OF THE CALCITARCH GENUS *PITHONELLA* BASED ON EXQUISITELY PRESERVED TURONIAN MATERIAL FROM TANZANIA

JENS E. WENDLER,[1,2] INES WENDLER,[1,2] AND BRIAN T. HUBER[1]
[1]Smithsonian Institution, NMNH, Department of Paleobiology, P.O. Box 37012, Washington DC, 20013-7012, USA; and [2]Bremen University, Geoscience Department, P.O. Box 330440, 28334 Bremen, Germany, <wendler@uni-bremen.de>

ABSTRACT—Extraordinarily well-preserved pithonellid microfossils (calcitarchs, "calcispheres") from the Turonian (upper Cretaceous) of Tanzania reveal previously unknown morphological traits, crystallographic patterns, and chemical signatures, providing new insight to this enigmatic group of microfossils. Using combined transmitted-reflected light microscopy, scanning electron microscope imagery, electron microprobe elemental analysis and stable isotope geochemistry, the present study reveals four new aspects of the genus *Pithonella*, notably, the following. An affinity with cyst-forming organisms, potentially the dinoflagellates, is indicated by the presence of a hatch opening and corresponding operculum. The pristine outer wall architecture consists of thin, smooth shingle-shaped plates with regular rows of slit-shaped pores and an apical sub-angular or circular pore. This primary surface pattern is significantly different from previous descriptions of an outer wall consisting of "parquet-shaped" prismatic crystal rows; this latter surface pattern is formed by secondary overgrowth. The crystallographic pattern of the inner wall is crypto-crystalline. Unaltered pithonellids reveal a calcite chemistry characterized by comparably high Mg-contents, relatively enriched stable carbon isotope values, and stable oxygen values indicating a surface water habitat. Based on these previously unseen traits, the diagnosis of the genus *Pithonella* is emended. A new species, *Pithonella diconica*, is described from the lower-middle Turonian sediments of Tanzania.

INTRODUCTION

THE TAXONOMY of Cretaceous pithonellid calcitarchs ("calcispheres" with radial, uniformly inclined wall crystals, Versteegh et al. [2009]) is ambiguous and, therefore, their paleoecological and biostratigraphic applicability have been limited despite their widespread distribution. In early studies these mostly spherical calcareous microfossils were associated with the benthic foraminiferal genus *Lagena* (Kaufmann, 1865). Pithonellid calcitarchs were thought to belong to various groups of foraminifera, including *Oligostegina*, *Fissurina*, *Orbulinaria*, *Pleurozonaria*, *Stomiosphaera,* (Colom, 1955) and other speculation placed them into tintinnida, calcareous algal spores, chlorophycean algal zoospores, unicellular algae, benthic algal oogonia, oolitic structures, protozoa, planktonic protists, planktonic ciliate organisms (as summarized by Dias-Brito, 2000). Even in the more recent literature focusing on carbonate geology (Farzadi, 2006; Piryaeu et al., 2011) the term *Oligostegina* is still in use for pithonellid microfossils. Conservative classifications have designated the genus *Pithonella* as Calcisphaerulidae *incertae sedis* for several decades (Lorenz, 1902; Masters and Scott, 1978; Villain, 1975; Villain, 1977) and currently the group is transferred to the new Incertae sedis group of the Calcitarcha (Versteegh et al., 2009). Alternative classifications were summarized by Masters and Scott (1978), who provided a microstructure-based classification of genera and families of the Mesozoic "calcispheres". These authors stress the strong affinity of some pithonellid forms with reproductive cysts of modern algae including calcareous green dasyclad algae, and also suggest a possible affinity with dinoflagellates. Comparison and systematic work on Deep Sea Drilling Project (DSDP) material (e.g., Bolli, 1974; Fütterer, 1984), with emphasis on the wall-crystal structure and rare findings of dinoflagellate tabulation (morphological terms are presented in Fig. 1), led to the proposal that a majority of Mesozoic calcispheres with an oblique and radial wall type, and some pithonellid forms as well, are similar to calcareous cysts formed by modern dinoflagellates. This systematic affiliation is supported by the presence of an archeopyle (hatch opening), distinct to subtle (sometimes ambiguous) tabulation and comparable size (Dali-Ressot, 1987; Keupp, 1981; Keupp, 1987; Keupp and Kienel, 1994; Keupp et al., 1991; Villain, 1981; J. E. Wendler and Willems, 2004; Willems, 1990; Young et al., 1997; Zügel, 1994). Dinoflagellates that form calcareous cysts as resting/reproductive or coccoid stages of their life cycle (calcified diploid and haploid phase, respectively [Meier et al., 2009]) belong to the Family Thoracosphaeraceae (Elbrächter et al., 2008) and previously were grouped with the Peridiniaceae, Subfamily Calciodinelloideae (Fensome et al., 1993). The motile cells consist of plates arranged in a taxonomically significant order, the peridinialean tabulation (Fig. 1.1a–1.1c), which may or may not be reflected in the corresponding cysts (Fig. 1.3, 1.4). In many cysts this pattern is only reflected in the shape of the archeopyle (Fig. 1.2). The archeopyle is opened by detaching a lid-like part of the cyst, the operculum (Fig. 1.2, 1.3, 1.5, 1.6), which includes one or several plates and often represents the 3′ plate (Fig. 1.1a). Due to its distinct relation to the tabulation, the shape of the archeopyle, or of the operculum in closed cysts, represents a taxonomic key trait that characterizes a dinoflagellate-nature of cyst-like microfossils (Streng et al., 2004).

Pithonellid calcitarchs first appeared in the Barremian and are major, often rock-forming, components of many upper Cretaceous deposits. The group reached its highest diversity during the Cenomanian through Coniacian (Dias-Brito, 2000), significantly declined towards the end of the Cretaceous, and became extinct at, or possibly just after, the Cretaceous–Paleogene boundary (Dias-Brito, 2000; Kienel, 1994; J. E. Wendler and

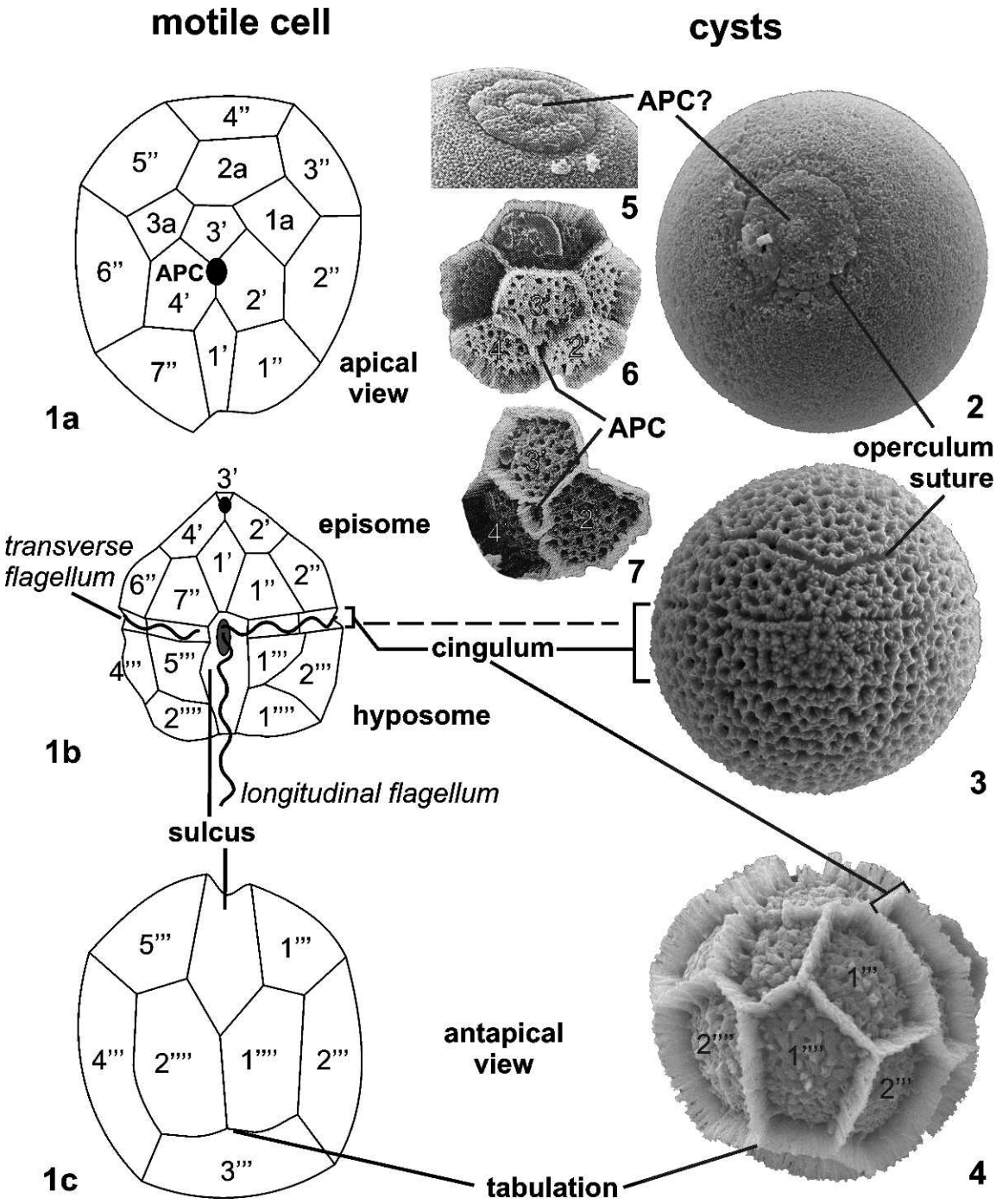

FIGURE *1*—Sketch of principle peridinialean tabulation in motile dinoflagellate cells (left panel), and its expression in the corresponding cysts (right panel): *1a,* apical view; *1b,* ventral view; *1c,* antapical view; APC=apical pore complex; *2–4*, cysts from dinoflagellates living in the culturing facility of Bremen University: *2*, *Leonella granifera* (Fütterer, 1977) Janofske and Karwath *in* Karwath, 2000, a modern cyst without tabulation patterns, apical view showing an operculum and a central knob (observed in two of five analyzed cysts); *3*, *Calciodinellum operosum* showing weak tabulation (dorsal view); *4*, *Calciodinellum operosum* (Deflandre, 1947) showing strong tabulation (oblique antapical view); *5*, *Leonella granifera* from Quaternary sediments, image modified from (Höll et al., 1998, p. 7, pl. I, fig. 2) showing a distinct knob with central depression that probably reflects the APC within the operculum; *6*, *Calciodinellum operosum*, entire detached multiple-plate operculum with expression of the APC, modified from Kerntopf (1997, pl. 23, fig. 1); *7*, *Calciodinellum operosum*, partial operculum showing reflection of the apical pore in the middle between plates 2′, 3′, and 4′, modified from Kerntopf (1997, pl. 23, fig. 3).

Willems, 2002). The two dominant species of the Cretaceous, *Pithonella sphaerica* and *Pithonella ovalis*, comprise the majority of the so-called “calcispheres” reported in the Cretaceous literature (Dias-Brito, 2000 and references therein). Analogous to many Thoracosphaeraceae, pithonellids are remarkably featureless and don’t show clear tabulation. Previous to this study, they generally have been found with a very small opening that is difficult to associate with an archeopyle or operculum because it is smaller than any archeopyles of modern calcareous dinoflagellate cysts. Additionally, this opening may be diminished in size by diagenetic crystal growth. Furthermore, calcareous dinoflagellate cysts

https://doi.org/10.1666/12-121 Published online by Cambridge University Press

TABLE 1—Overview of morphological characteristics arguing for or against the affiliation of pithonellids with dinoflagellates and possible alternatives; dinocyst=calcareous dinoflagellate cyst.

Feature	Pro dinoflagellates	Contra dinoflagellates	References	Opposing comments	References
Peridinoid tabulation		Not observed for *Pithonella* spp.	Streng et al. (2004); Versteegh et al. (2009)	Recent *L. granifera* and *T. heimii* and most fossil oblique- and ortho- wall type dinocysts lack tabulation	Janofske and Karwath (2000); e.g., Keupp (1981)
	Tetratropis corbula is pithonellid and is tabulated		Wendler and Willems (2004); Willems (1990)	*Tetratropis* is associated with microfossils not considered to be dinocysts, or tabulation is thought to represent ornamentation	Odin (2011); Versteegh et al. (2009)
	Sub-angular apical suture		This study	Could reflect penta- / hexa-radial symmetry unrelated to tabulation	
Operculum/ archeopyle		Only a small pore-like hole observed	Zügel (1994); Versteegh et al. (2009)		
	Suture and "apical disk" (=operculum) in *Pithonella* spp.		Zügel (1994); Masters and Scott (1978); This study		
		Central pore	This study	Possible analogue: central knob in operculum of modern *L. granifera*; Opercula of *P. lamellata, P. atopa* and *Pirumella* sp. (dinocyst) also have a central pore	This study
		Only found closed in *P. sphaerica* and *P. ovalis*	e.g., Zügel (1994); This study	Secondary openings within operculum area are known from *Calcicarpinum bivalvum*	Versteegh (1993)
	Also found open in *P. lamellata, P. atopa* and in *Pithonella* sp. 1		Keupp and Kienel (2004); This study		
Spherical endocoel		Various shapes in pithonellids	Versteegh et al. (2009)	Some dinocysts, e.g., *Pirumella krasheninnikovii* / *O. collaris* have an ovoid / flattened, resp. endocoel	Wendler et al., 2001
Antapical pore		Present in *Pithonella* but not known from dinocysts	Villain (1977); This study		
Pores	Present in *Pithonella* (and in Recent *S. albatrosianum*)		Keupp and Kienel (1994); This study		
Biomineralization	Similar model for *Pithonella* as for Recent dinocysts		Keupp and Kienel (1994); This study		
	Wall composed of minute crystals similar to Recent *L. granifera*		This study	Most other dinocyst species have a less complex wall structure composed of larger crystals	
$\delta^{13}C$		Higher than co-occurring planktic foraminifera (unlike modern *T. heimii* and fossil *Pirumella krasheninnikovii* and *Orthopithonella*? *globosa*)	This study; Kohn and Zonneveld (2010); Friedrich and Meier (2003)	No data available for modern dinocysts other than *T. heimii,* which is a coccoid vegetative stage and not a sexual reproductive cyst	
Alternative affinity of pithonellids		Dasycladaceae (Similarity in size and possibly $\delta^{13}C$)	Masters and Scott (1978); Wefer (1985); This study	*Pithonella* is not typical for shallow-water habitat; *Pithonella* is not aragonitic	Wendler et al. (2002a); Dias Brito (2000); this study
		Tintinnideae	Villain (1975, 1977)	No mineralized tests known	
		Calpionellids (spiral wall structure)	Villain (1975)	*Pithonella* does not have a vase-like morphology, known Calpionellids restricted to late Jurassic to lowermost Cretaceous	

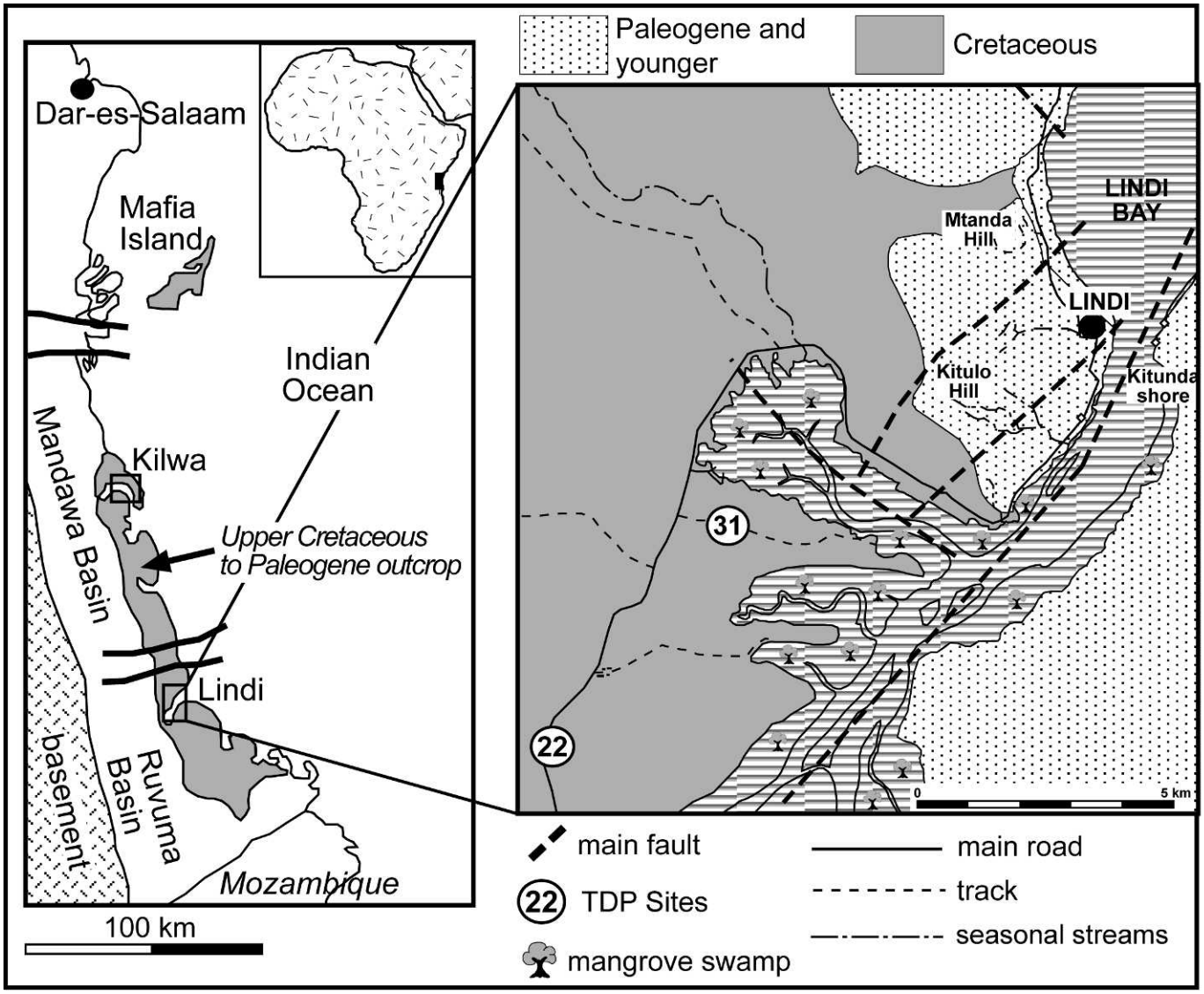

FIGURE 2—Map of research area and location of Tanzania Drilling Project drill Sites discussed in this study.

mostly have a spherical interior (endocoel) independent of their outer shape (except for ovoid forms like *Pirumella krasheninnikovii* or the apically flattened *Orthopithonella* (?) *collaris* (J. E. Wendler et al., 2001) whereas the central cavities of pithonellid forms follow any of the often non-spherical outer shapes. Recent publications that recognize the archeopyle as a key trait of dinoflagellate taxonomy with higher significance than the often equivocal wall-structure have cast doubt on an association of pithonellid calcitarchs with dinoflagellates (Elbrächter et al., 2008; Fensome et al., 1993; Streng et al., 2004; Versteegh et al., 2009). Further complication in the taxonomy of this group arose from an isolated observation of densely packed specimens that may be interpreted as colony formation in the pithonellid genus *Bonetocardiella* (Villain, 1975)—a life strategy not known among modern dinoflagellates. Also the pithonellid genus *Tetratropis* appears to be related to the so-called gilianelles that are not regarded to be dinoflagellates (Odin, 2011). These ambiguities result in a dilemma where, on the one hand, the pithonellid calcitarchs would be stratigraphically and paleogeographically widespread enough (Dias-

→

FIGURE 3—Opercula of *Pithonella* from Tanzania Drilling Program Sites 22 and 31. *1a–c, Pithonella sphaerica* in slightly oblique apical view: *1a*, combined reflected and transmitted light, operculum is visible as a bright subangular (pentagonal or hexagonal) area, a nook to the upper left suggests a composite of multiple plates; *1b*, second combined reflected and transmitted light view with light source rotated ~180° showing the central pore and light transmission opposite to *1a* with the operculum darker than the rest of cyst body; note rows of the parallel surface crystallites; *1c,* SEM image, the operculum that is optically visible in *1a* and *1b* is invisible and not morphologically reflected on the surface of the inner wall (outer wall is missing; arrow points to apical pore); *1d* scheme of operculum (white) and fitted circle (black) reveals sub-angularity; *2a–c, Pithonella sphaerica* apical view: *2a*, SEM image revealing the operculum suture as a thin line in the outer wall enhanced by slight overgrowth; *2b,* light-optical image, note that, unlike in *1a* and *1b*, rows of pores are barely light-optically visible when the outer wall is present; *2c,* close-up of sub-angular operculum suture and apical pore; *2d* scheme of operculum (white) and fitted circle (black) reveals sub-angularity. All scales=50 μm.

https://doi.org/10.1666/12-121 Published online by Cambridge University Press

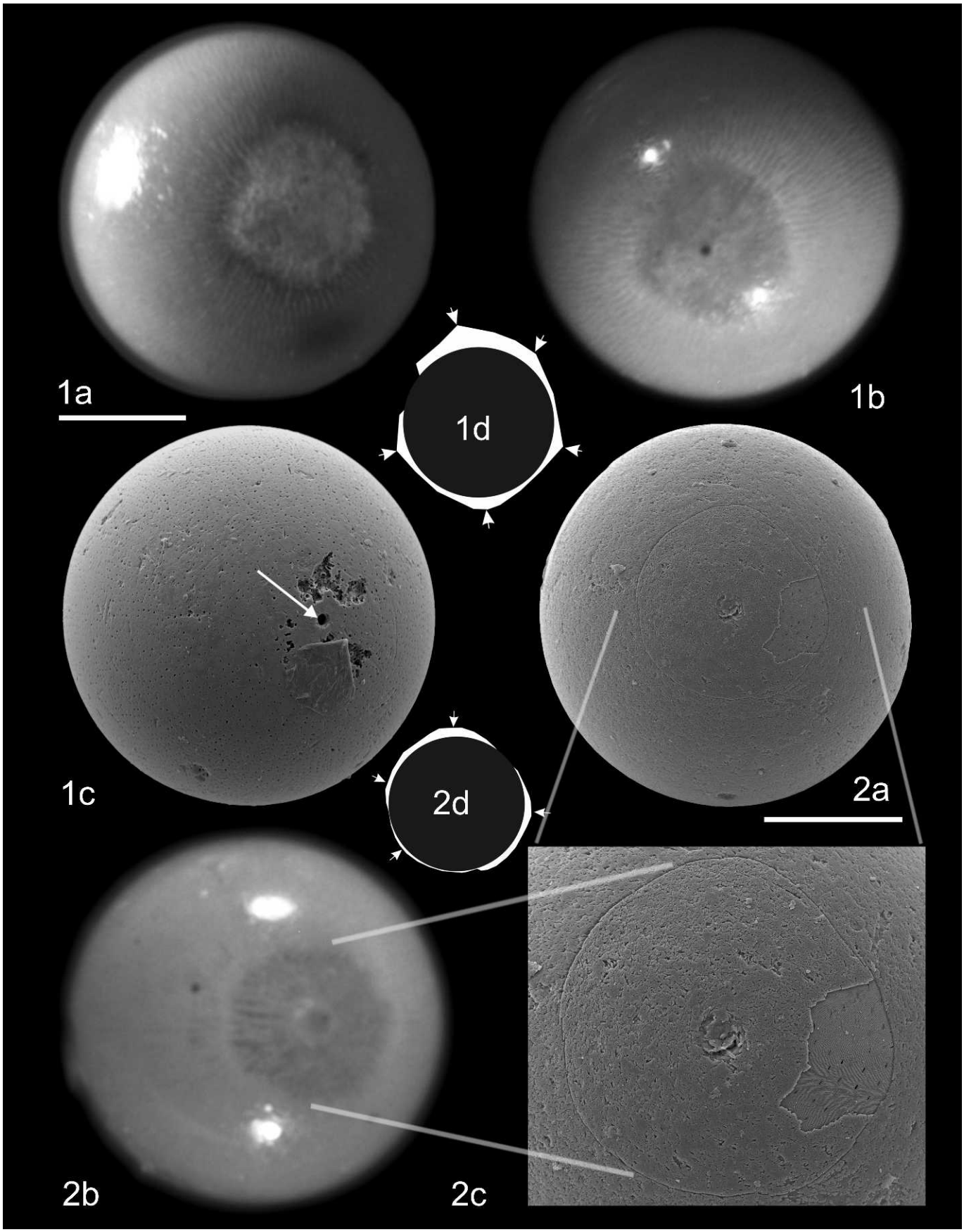

https://doi.org/10.1666/12-121 Published online by Cambridge University Press

Brito, 2000) to be potentially applied as paleoenvironmental indicators (J. E. Wendler et al., 2002b) but, on the other hand, their biology and ecology have been largely unknown.

Here we report on detailed observations of opercula in the genus *Pithonella* providing a compelling argument that pithonellid calcitarchs showing this feature represent fossils of cyst-forming organisms, potentially of dinoflagellates. The terms cyst and operculum are used to describe the studied specimens throughout this paper as both terms are not restricted to dinoflagellates. An overview of the complex issue of possible affiliations of the group, including the controversies and the novel interpretative paths facilitated by the present study are summarized in Table 1.

The studied material comes from Tanzanian sediments of Turonian age (89–93 Ma), which were initially targeted for their exceptional preservation of unaltered foraminifera calcite and used to generate high quality geochemical paleoclimate proxy records (MacLeod et al., in press; I. Wendler et al., 2011). The present study documents the first observation of pristinely preserved Late Cretaceous pithonellids, which allows for a detailed description of previously unknown morphological wall architectural traits. Furthermore, the excellent preservation allows for geochemical analyses of the cyst wall in order to determine its elemental and stable isotopic composition.

MATERIAL AND METHODS

This study is based on specimens recovered from two boreholes drilled during the 2007–2008 phase of the Tanzanian Drilling Project (TDP). TDP Site 22 was drilled at 10°04′39.4″S/39°37′33.5″E (Fig. 2) and comprises the lower through middle Turonian upper *Whiteinella archaeocretacea* and the *Helvetoglobotruncana helvetica* planktic foraminiferal biozones (Jiménez Berrocoso et al., 2010). Site TDP31 is located at 10°01′49.9″S/39°38′44.0″E and comprises the early to late Turonian *Hv. helvetica* through *Dicarinella concavata* planktic foraminiferal biozones (Huber and Petrizzo, in press). The sediments are unconsolidated clay- and siltstones with a carbonate content typically ranging from 10–15 wt.% (Jiménez Berrocoso et al., 2012) and they were deposited in an upper slope to outer shelf paleo-depth (I. Wendler et al., 2011). Samples were disaggregated in tap water and the size-fractions were separated over 20, 63, 125 and 250 μm sieves. Specimens were picked from the 20–63 μm fraction with an eyelash attached to a pen. Sample notation, such as TDP22-20-1 (20–30 cm), describes site number, core number, and core-section with cm-interval. SEM stub numbers, e.g., TDP22-31-1_H4 (20–30 cm), contain the sample number and end with the stub grid (A to K) location, and the cm interval following in brackets. Stubs and further specimen location information are on file at the Smithsonian Institution.

Optical images were taken at approximately ×100 magnification using a Nikon SMZ1500 binocular light microscope and multiple-plane integrated imaging with NIS Elements™ imaging software. Optical investigation with polarized light was achieved with a Leitz Ortholux binocular microscope on the same specimens that were then transferred to stubs for scanning electron microscope (SEM) analysis on a Phillips XL-30 ESEM with a LaB6 electron source. Calcite chemistry was measured on polished individual microfossil specimens embedded in epoxy using a JEOL 8900 electron microprobe (EMP) wavelength dispersive system (WDS) analysis with five spectrometers and the analytical software PROBE FOR WINDOWS™. The microprobe was operated at 13 kV, 15 nA with a beam size of 3 μm. Standardization is based on the Smithsonian Institution standards for calcite (USNM 13621), dolomite (USNM 10057), manganite (USNM 157872), and strontianite (USNM R10065). Contents of MgO, FeO, CaO, SrO, and MnO are reported as wt. %, and detection limits are 100 ppm (Mg), 200 ppm (Fe), 200 ppm (Ca), 100 ppm (Sr), 300 ppm (Mn).

RESULTS AND DISCUSSION

The following descriptions focus on the species *Pithonella ovalis* and *Pithonella sphaerica*. Besides these dominant species the Tanzanian assemblage comprises *Pithonella perlonga* Andri 1972*, Pithonella trejoi* Bonet 1956*, Pithonella discoidea* Willems, 1992, a new form *Pithonella diconica* (this paper), *Pithonella microgranula* Zügel 1994=*Pithonella atopa* Keupp and Kienel 1994 and *Pithonella lamellata* Keupp and Kienel 1994; these species are included here to achieve a comprehensive description of the pithonellid structural features.

Shell architecture: apical disc–operculum.—The glassy preservation of the Tanzanian material allows for detailed observation using combined transmitted and reflected light. With this kind of illumination a disk-like structure is visible as an area that transmits light differently from the cyst body (Fig. 3.1a, 3.1b, 3.2b). In SEM imaging, this area appears encircled by a thin suture line in the outer wall layer (Figs. 3.2a, 3.2c, 4.1–4.3). The

→

FIGURE 4—Opercula characteristics and appearance in various preservation stages, comparison with other species. *1, Pithonella sphaerica*, apical view showing the operculum and central apical pore on the inner wall surface; the operculum suture is marked by a line of dissolution and cracks along the crystal-inclination change, the outer wall is partly present (smooth areas); *2, Pithonella sphaerica*, local dissolution reveals tube-like appearance of the pores, zoomed area shows crystal orientation change along the operculum suture, scale=50 μm; *3, Pithonella ovalis*, apical pore and operculum suture in slightly etched inner wall surface; *4, Pithonella ovalis*, apical pore revealing a clearly defined rim, scale=5 μm; *5, Pithonella ovalis*, operculum directed to the upper left, partial etching along the rim reveals apically inclined crystal orientation in the operculum as opposed to the antapically inclined crystal orientation in the cyst body; *6, Pithonella lamellata*, operculum viewed from the cyst inside, revealing a central pore and a less dense microstructure of the operculum compared to the cyst body, bright crystals are beginning secondary overgrowth; *7, Pirumella multistrata*, apical view of operculum and a central pore. All scales=10 μm unless noted otherwise.

→

FIGURE 5—Antapical pole. *1a, Pithonella ovalis*, scale=10 μm, slit-shaped antapical pore within an otherwise pore free area, outer wall largely preserved; note that most slit-pores appear closed by a thin cover; *1b*, detail of antapical pore, scale=2 μm; *2, Pithonella ovalis*, antapical wall section showing the antapical pore widening towards the cyst inside, scale=5 μm; *3,* antapical pore on inner wall surface, scale=10 μm; *4a, b, Pithonella sphaerica*, view from inside the cyst on antapical pole, showing that antapical pore is slightly larger than the other pores, scales are 2 μm and 10 μm, respectively; *5, Pithonella ovalis*, antapical pore on excellently preserved cyst surface, note shingle-like structure of the outer wall and that the antapical pore is thinly covered (organic membrane or calcite film?), scale=2 μm; *6, Pithonella ovalis,* elongated antapical pore and shingle-like structure of outer wall, scale=5 μm; *7, Pithonella ovalis,* view on antapical cyst pole in exquisite preservation reveals plate-like sutures in cyst surface and barely visible, covered antapical pore (arrow), scale=5 μm.

https://doi.org/10.1666/12-121 Published online by Cambridge University Press

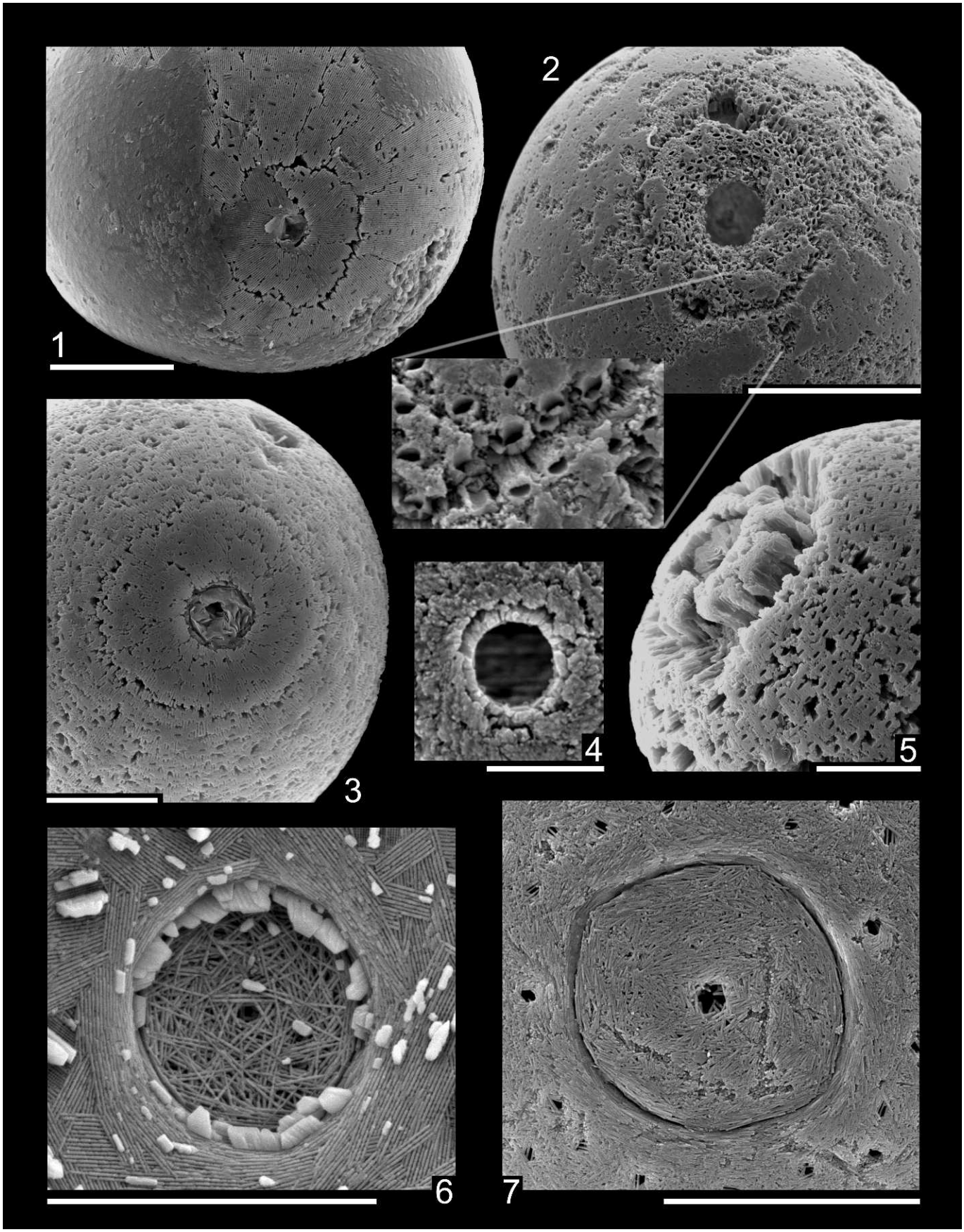

https://doi.org/10.1666/12-121 Published online by Cambridge University Press

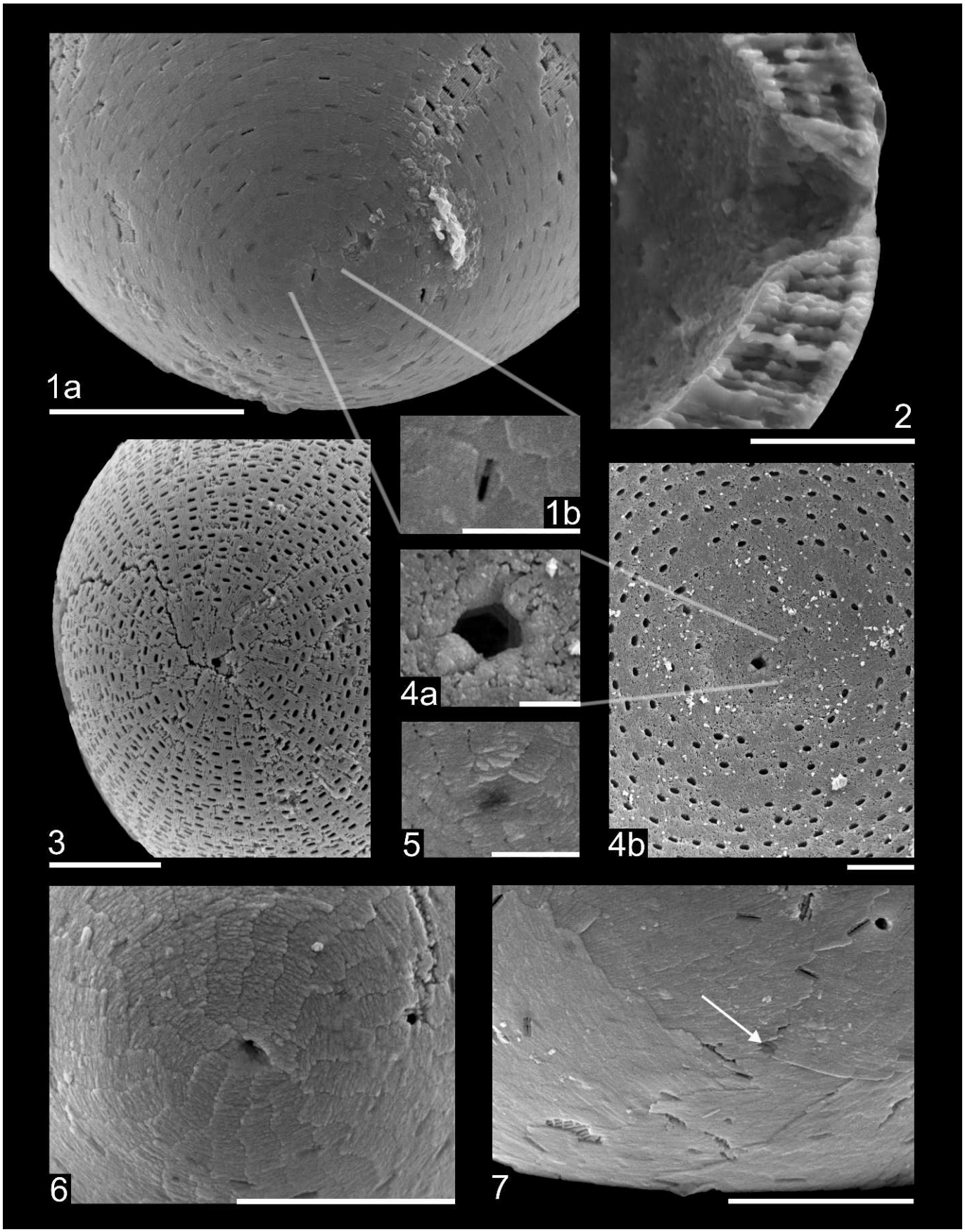

https://doi.org/10.1666/12-121 Published online by Cambridge University Press

suture and the differing light-optical appearance originate from a slight change in the crystal inclination (inner and outer wall) between this apical disc and the remainder of the cyst; along the suture, the crystals of the cyst body that are inclined in an antapical direction meet the crystals of the apical disk, which have a more radial or even apically orientated inclination (Fig. 4.2, 4.5). Notably, in SEM imagery the suture line of the apical disc is visible only rarely (Fig. 3.1c), most likely when a thin secondary overgrowth is developed (Fig. 3.2a, 3.2c) or slight diagenetic etching took place, both of which can reveal the suture line (Fig. 4.1–4.3). Natural etching additionally exposes the underlying crystal orientation change that distinguishes the apical disc from the cyst body (Fig. 4.2, 4.5).

Since the disc-suture often encompasses a sub-angular area (Fig. 3.1d, 3.2c, 3.2d) it could be interpreted to reflect an underlying tabulation that involves multiple plates, suggestive of a dinoflagellate operculum. The diameter of the apical disk varies from 10–65 μm, and is between one quarter and one half of the cyst diameter. The sub-angularity could reflect multiple plates (e.g., the plates 2′, 3′, 4′ of a peridinialean tabulation) (compare Fig. 1.1a, 1.7). Alternatively, the sub-angularity could simply reflect a penta- or hexa-radial symmetry. A pore in the center of the apical disc may be sub-angular or circular. This pore varies in diameter from 3–10 μm (compare Fig. 3.1b, 3.1c to 3.2a, 3.2c), and it can be up to one third of the size of the operculum (Fig. 4.1–4.3). It has a well-defined rim (Fig. 4.4). The apical pore obviously represents what has often been observed as the typical small opening of pithonellid cysts. The complex apical disk yields two potential openings of a pithonellid cyst: 1) the apical pore, and 2) the entire area within the operculum-suture. The whole operculum is, however, rarely found to be actually detached and secondary mechanical destruction can be difficult to be distinguished from a primary hatching structure due to the irregularity of the suture (Fig. 4.1–4.5). The apical pore was thought to be too small to function as an archeopyle (Streng et al., 2004; Versteegh et al., 2009).

Importantly, we discovered a similar operculum involving a central pore in the pithonellid species *Pithonella lamellata*, and in a species with oblique wall-architecture, *Pirumella multistrata* (Fig. 4.6, 4.7). Both species are represented in the Tanzanian material with an attached and detached apical disc, indicative of a function as hatch-opening in a cyst (Wendler and Bown, 2013). Because *Pirumella multistrata* is generally accepted as a calcareous dinoflagellate cyst based on its oblique wall-type, the similarity of its apical disc with that of the pithonellids (Fig. 4.6, 4.7) suggests interpretation of the pithonellid apical disc areas as a dinoflagellate operculum. An apical disc that is barely visible in occasional specimens of *P. sphaerica* from chalk facies has been mentioned previously by Zügel (1994, p. 120, pl. 1, fig. 7). Despite strong secondary alteration, its architecture is the same as in the Tanzanian material with a pore in the middle—a fact that has motivated Zügel (1994) to reject the interpretation of the apical disc as an operculum. The present evidence of opercula in pithonellids reveals that they likely functioned as cysts. The described opercula of *P. lamellata, P. multistrata, P. sphaerica* and *P. ovalis* have in common the previously undescribed feature of the central pore. A possible analogue to this apical pore can be observed in the modern species *Leonella granifera* (Fig. 1.2, 1.5; see also Janofske [1996], p. 299, pl. 1, fig. 1a; Janofske and Karwath [2000], p.113, pl. 2, fig. 25; Kerntopf [1997], pl. 32, figs. 5, 6), which also yields a central feature in the form of a knob with central depression, and in *Caliodinellum operosum* where the apical pore is fully reflected on the cyst (Fig. 1.6, 1.7). This analogy suggests that the central pore of pithonellid opercula represents an explicit dinoflagellate trait, rather than providing argument against their affiliation with dinoflagellates.

Another pore with an unknown function commonly exists in antapical position (Fig. 5). In a wall cross-section it forms a funnel-like structure that opens towards the inside of the cyst (Fig. 5.2). While openings on both sides of *P. ovalis* have previously been attributed to secondary break-up (Keupp, 1987) due to wall thinning at the cyst poles, the exquisite preservation of the Tanzanian material enables a detailed morphologic characterization of multiple intact specimens and reveals that antapical pores clearly represent a primary, well-constructed pore rather than a secondary hole (Fig. 5.1, 5.2, 5.4–5.7). The presented evidence supports earlier reports of a possible antapical opening (Villain, 1977).

Wall architecture: slit-pores and inner wall.—The wall architecture shows a radial, uniformly inclined crystallographic orientation (Fig. 6.1b) and a system of slit-shaped pores (Fig. 6.1c). Pores in *Pithonella* spp. were first suspected by Keupp and Kienel (1994) but a lack of pristine material hindered a detailed study. The pore system reveals an antapically directed, inclined (pithonellid) orientation relative to the cyst surface in alignment with the crystallographic orientation. The pores can be traced through the cyst wall to the inner surface (Fig. 6.2–6.5). The inner wall is 2–18 μm thick in equatorial position and varies with the specimen diameter (~1/10 cyst diameter)—likewise the wall thickness varies in elongated species, like *Pithonella ovalis,* by a

→

FIGURE 6—Wall architecture, inner wall. *1a–c, Pithonella sphaerica*, scale=20 μm: *1a*, transmitted light, dark line marks operculum suture, bright spot is the apical pore; *1b,* longitudinal cross-section in polarized light showing skewed axis cross indicative of radial-inclined (pithonellid) crystal orientation; *1c,* backscattered electron microscopic image of polished thin section illustrating antapically inclined orientation of dense pore system (apical pole at the top); *2, Pithonella ovalis*, longitudinal cross-section showing inclined pore system, note variable wall thickness thinning at the cyst poles (apical pole to the left), scale=10 μm; *3, Pithonella sphaerica,* "cigar-shaped" pores (conical decrease in pore width towards cyst surface) in latitudinal cross-section, enlarged inset shows striated microgranular surface, scale=5 μm; *4, Pithonella sphaerica*, latitudinal cross-section (parallel to slit-pores) showing fan-shaped wall-crystal arrangement; note homogeneous appearance at bottom of the image where the wall is broken in longitudinal direction (vertical to slit-pores) as in *5*, scale=5 μm; *5, Pithonella ovalis,* longitudinal cross-section (vertical to slit-pores) showing homogenous appearance of the micro-crystalline wall, scale=5 μm; note cobble-like crystal ends on inner cyst surface in *4* and *5*.

→

FIGURE 7—Wall architecture, outer wall. *1, Pithonella ovalis*, longitudinal cross-section of antapical part showing both homogenous, crypto-crystalline wall appearance, and laminated multi-layered structure revealed upon initial recrystallization; *2, Pithonella sphaerica,* apical pore wall revealing the original laminated architecture of the inner wall (outer wall is missing); *3, Pithonella ovalis*, oblique lateral-antapical view, pristine specimen with smooth outer surface and regular longitudinal rows of slit-pores, scale=10 μm; *4, Pithonella ovalis*, the thin outer wall is sharply separated from the inner wall, shingle-shaped crystallite plates (marked) are arranged in longitudinal rows; note rod-shaped crystallites on inner wall surface; *5, Pithonella ovalis*, slit-pores in well preserved outer wall (detail of specimen in *3*); *6, Pithonella sphaerica*, thin, veneer-like outer wall and underlying inner wall surface with parallel rod-shaped crystallites oriented in two directions. All scales=5 μm unless noted otherwise.

https://doi.org/10.1666/12-121 Published online by Cambridge University Press

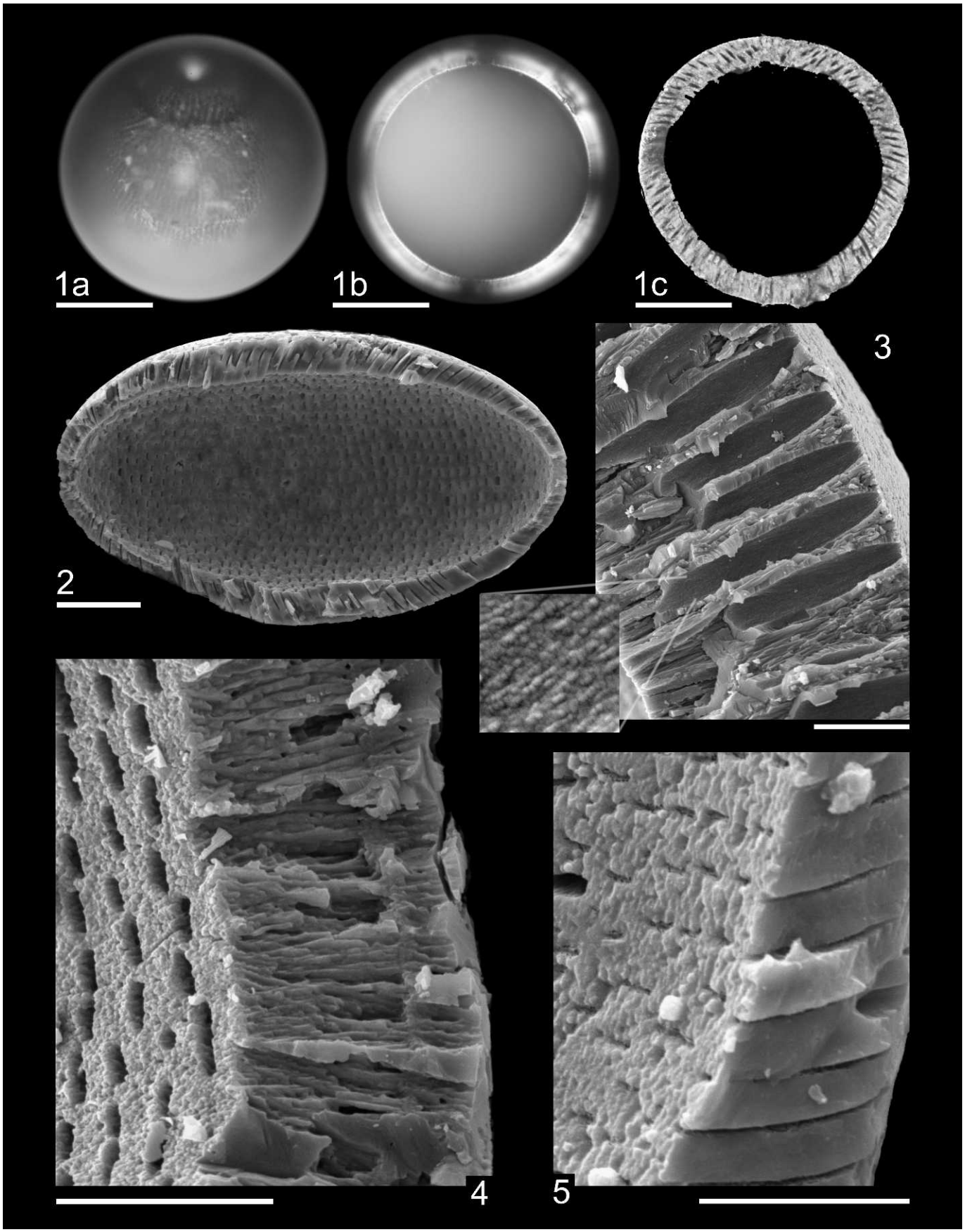

https://doi.org/10.1666/12-121 Published online by Cambridge University Press

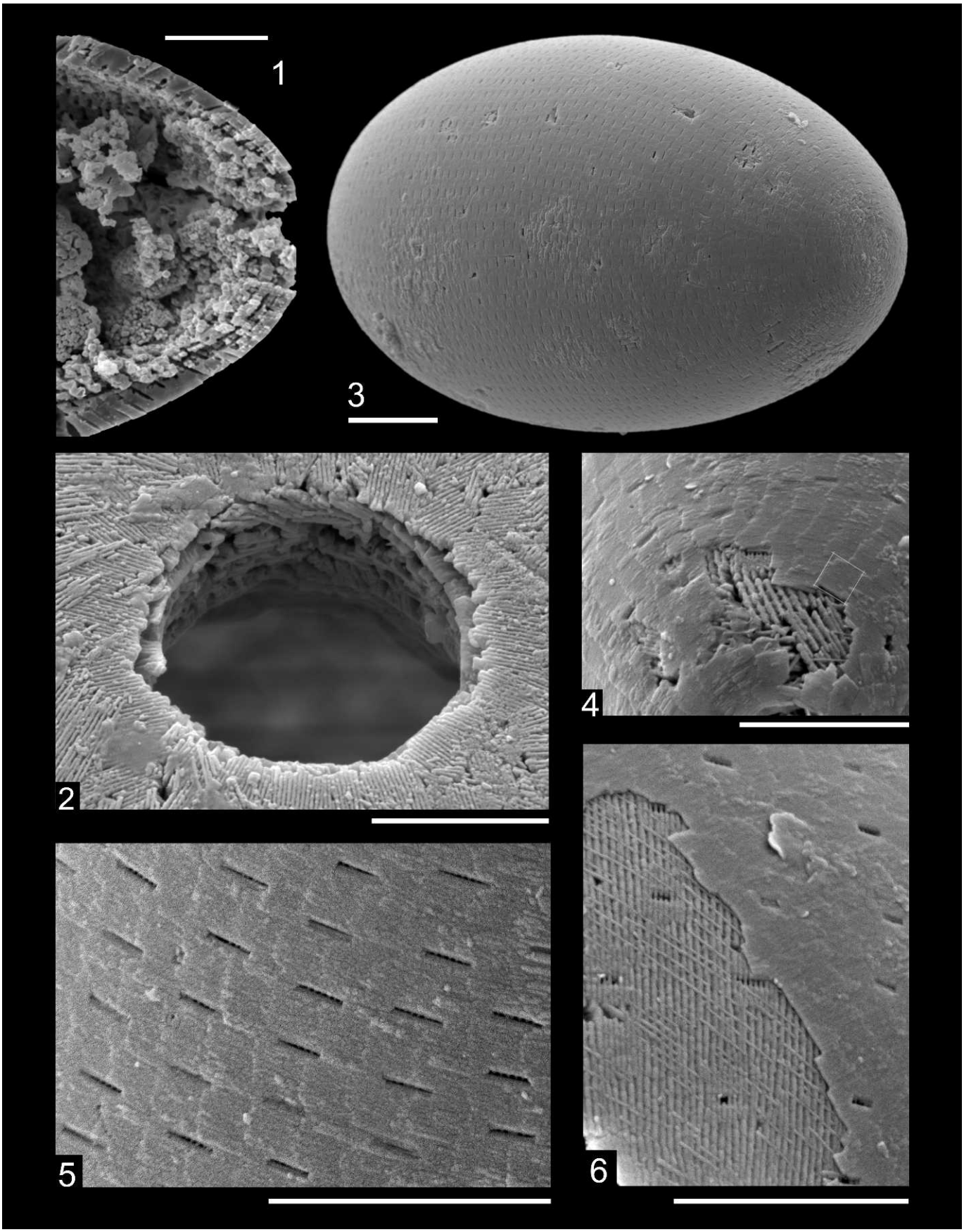

https://doi.org/10.1666/12-121 Published online by Cambridge University Press

factor of two from the equator (thickest) to the poles (thinnest). It is crypto-crystalline and in longitudinal cross-section appears as a compact mass (Fig. 6.2, 6.5). In latitudinal cross-section, a fan-shaped stacking of multiple nanno-scale crystals can be observed (Fig. 6.4). Some specimens reveal the compact crypto-crystalline wall appearance and, in other parts, a multiple nanno-crystal layering of the wall (Fig. 7.1). A laminar construction of the cyst wall is also evident in the rim of apical pores (Fig. 7.2). Such occasional occurrence of multi-layering in *P. ovalis* was first reported by Zügel (1994, pl. 1, fig. 5; pl. 2, fig. 9), who interpreted it as intra-species ecological variability. Our observations show that nanno-scale layering is inherent in the crypto-crystalline structure. The minute crystals constituting the inner wall are also visible on the walls of the slit pores (detail in Fig. 6.3). In specimens where the outer wall is missing the rows of pores are visible with light microscopy as a fine striation of dark lines (Figs. 3.1, 6.1).

Wall architecture: outer wall and detailed pore observations.—Figure 7.3 shows a pristine *Pithonella ovalis* with a remarkably smooth surface. The outer wall is constructed of parallel, longitudinally oriented rows of smooth, shingle-shaped crystallite-plates of size ~0.8 × 0.8 μm (Fig. 7.4). The slit pores on the outer wall are also arranged in these rows and form very thin slits (Fig. 7.5). The outer wall covers the cyst like a veneer with a thickness of only ~0.1 μm (Fig. 7.6). This new insight into the outer wall character necessitates revision of the existing outer wall definition; diagenetic growth of the sub-micron crystallites gradually creates the prismatic surface crystals which finally form the known parallel rows (see discussion on preservation).

On the outer wall the slit pores are very narrow, rectangular and have a well-defined rim formed by two rod-shaped crystallites (Fig. 8.4, 8.5), which have a different orientation than the rod-shaped crystallites covering the surface of the inner wall (Fig. 8.6, 8.8). In the best preserved specimens the pores appear to be covered by a thin final surface layer (Fig. 8.2, 8.3). On the inner wall surface the pores are wider and oval-shaped and are covered by rod-shaped crystallites in a grid-like manner (Fig. 8.6, 8.8), which are thinning across the pores (Fig. 8.6, 8.8) and can be visible through the thin slit in the outer wall (Fig. 8.5). Inside the cyst, the pores are wider and open (Fig. 8.1). The surface of the inner wall shows two layers of rod-shaped crystallites that can be interwoven (Fig. 8.9) or in two separate planes (Fig. 8.6), and have a different orientation around and between pores (Fig. 8.7–8.9). A notably higher crystal density surrounding the pores (Fig. 8.11) is visible in the crystallite cleavage in wall section (Fig. 8.10) and on etched surfaces causing a tube-like appearance (Fig. 8.12, 8.13).

Principle architecture.—The scheme in Figure 9.1 summarizes the principle cyst surface elements. The distal surface of the inner wall shows two layers of rod-shaped, parallel crystallites 0.15 to 0.3 μm wide, with a difference in angle of about 55° in their orientation and with specific orientation at the slit pores (Figs. 8.6–8.9, 9.4). In some specimens one direction is dominant while the other is strongly reduced (Fig. 8.11). Around the cyst poles these rod-shaped crystallites are arranged spirally (Fig. 9.3, 9.5). Interestingly, the direction of the spiral pattern switches between adjacent wall-layers (Fig. 9.3, 9.4). This change of orientation in the surface-crystallite-arrangement causes a ply-like, spiral architecture through the different layers of the inner wall (Fig. 9.1). A spiral orientation around cyst poles is also reflected in the arrangement of the starting points of slit pore rows (Fig. 9.5). Some specimens have an apparent reduced pore density near the poles (Fig. 9.6), although slit pores are a general feature of the operculum (Fig. 4.2).

Preservation.—In contrast to chalk and many other Cretaceous rocks that yield frequent pithonellid calcitarchs, the Tanzanian clayey silts provide a rare window that reveals gradual transitions between preservation stages from nearly pristine to overgrown (Fig. 10). The "best preserved end member" (Fig. 10.1) is a preservation state of *Pithonella* that has not been observed previously. It is characterized by the features newly described above under shell architecture. In Figure 10 we show a diagenetic path from pristine toward overgrown surfaces. The best preserved specimens are characterized by having a smooth surface formed by the shingle-like plates arranged in wavy, longitudinal rows (Fig. 10.1). In progressive diagenetic stages, partly overgrown surfaces develop (Fig. 10.4; see Figs. 11–13 for details). These transform to strong overgrowth (Fig. 10.7), and finally a parquet-pattern with parallel rows of idiomorphic crystals on the outer surface is formed (Fig. 10.9), and the latter represents strong secondary crystal growth and the appearance typically found in *Pithonella*.

The recrystallization path of the cyst-wall corresponds to those surface changes. The wall crystals in the pristine specimen (Fig. 10.2, 10.3) have a homogenous appearance suggestive of either 1)

→

FIGURE 8—Pores. *1, Pithonella ovalis*, pore system on the inner cyst surface, pores are wider than on the outer surface, scale=5 μm; *2, Pithonella ovalis*, slit pores on outer cyst surface are thinly covered at best preservation, scale=5 μm; *3–5,* details of slit-pores in outer wall of *Pithonella ovalis*, scales 1 μm, besides a thin cover (*3*) slit-pores have well-defined rims formed by two rod-shaped crystallites (*4, 5*), underlying grid-like crystallites of the inner wall are visible through the slit-pore in *5*; *6–9, Pithonella sphaerica*, details of microstructures around pores on inner wall surface showing two layers of parallel, rod-shaped crystallites, one of them covering the slit pores in a grid-like manner and with thinner crystallite diameter over the pores (*6* and upper left in *8*); the two layers can be in two separate planes (*6, 8*) or partly interwoven (*7, 9*); often a difference is observed in orientation of the rod-shaped crystallites in a rectangular field around the pores and between them (*7–9*); one of the two crystallites that border the slit-pore in the outer wall is preserved in *6* (lower left) and *8* (lower right); note its larger diameter and different orientation (parallel to the slit-pores) compared to the other crystallites (oriented diagonal to the slit-pores); scale in *6* and *8* is 5 μm, scale in *7* and *9* is 2 μm; *10, Pithonella sphaerica*, difference in cleavage between pore-wall crystals and wall substance between the pores, scale=5 μm; *11, Pithonella ovalis*, rod-shaped crystallites are denser around the pores than between them, scale=5 μm; *12, Pithonella sphaerica*, dissolution reveals denser pore-surrounding and results in tube-like structures, scale=10 μm; *13, Pithonella ovalis*, inner wall surface showing dissolution of less dense mineralized wall areas between the pores while crystallite-striation is still visible on the tube-like pores, scale=10 μm.

→

FIGURE 9—Summary of principle elements of operculum and cyst surface architecture. *1,* schematic overview of cyst surface elements around the operculum (detail of apical view, cyst diameter is larger than depicted area), long axes of slit-pores arranged spirally, in direction of their short axes pores form longitudinal rows; *2,* apical view of *Pithonella ovalis* showing surface elements in SEM-imaging, operculum is evident as a sharply bounded disc in the pristine outer wall (broken off along the suture line and partly missing on the right-hand side); *3, Pithonella ovalis,* penta-radial, spiraling wall-surface crystallite arrangement; *4, Pithonella sphaerica,* pores and rod-shaped crystallites on inner wall surface, note angle of ~55° in crystallite orientation between the two layers; *5, Pithonella sphaerica,* apical view on inner wall surface, spiral slit-pore arrangement, antapical pore (bright spot due to charging) is visible through the apical pore, both lath-shaped crystallites and rows of slit pores have a spiral orientation around the pole, with each next deeper layer crystallites switch orientation at an angle of ~55°; *6, Pithonella ovalis,* longitudinal arrangement of slit-pores and apical pore (outer wall is missing). All scales=10 μm.

https://doi.org/10.1666/12-121 Published online by Cambridge University Press

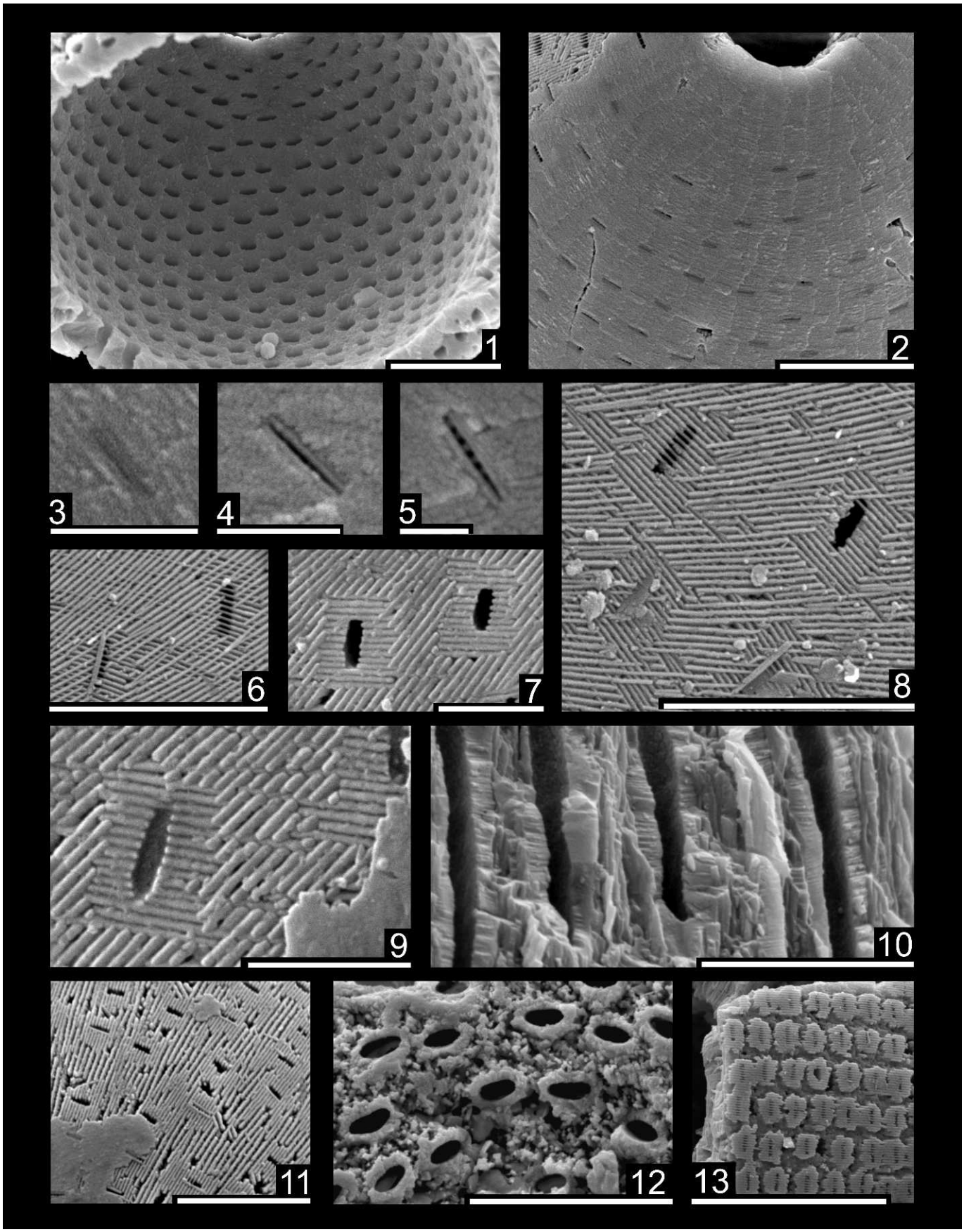

https://doi.org/10.1666/12-121 Published online by Cambridge University Press

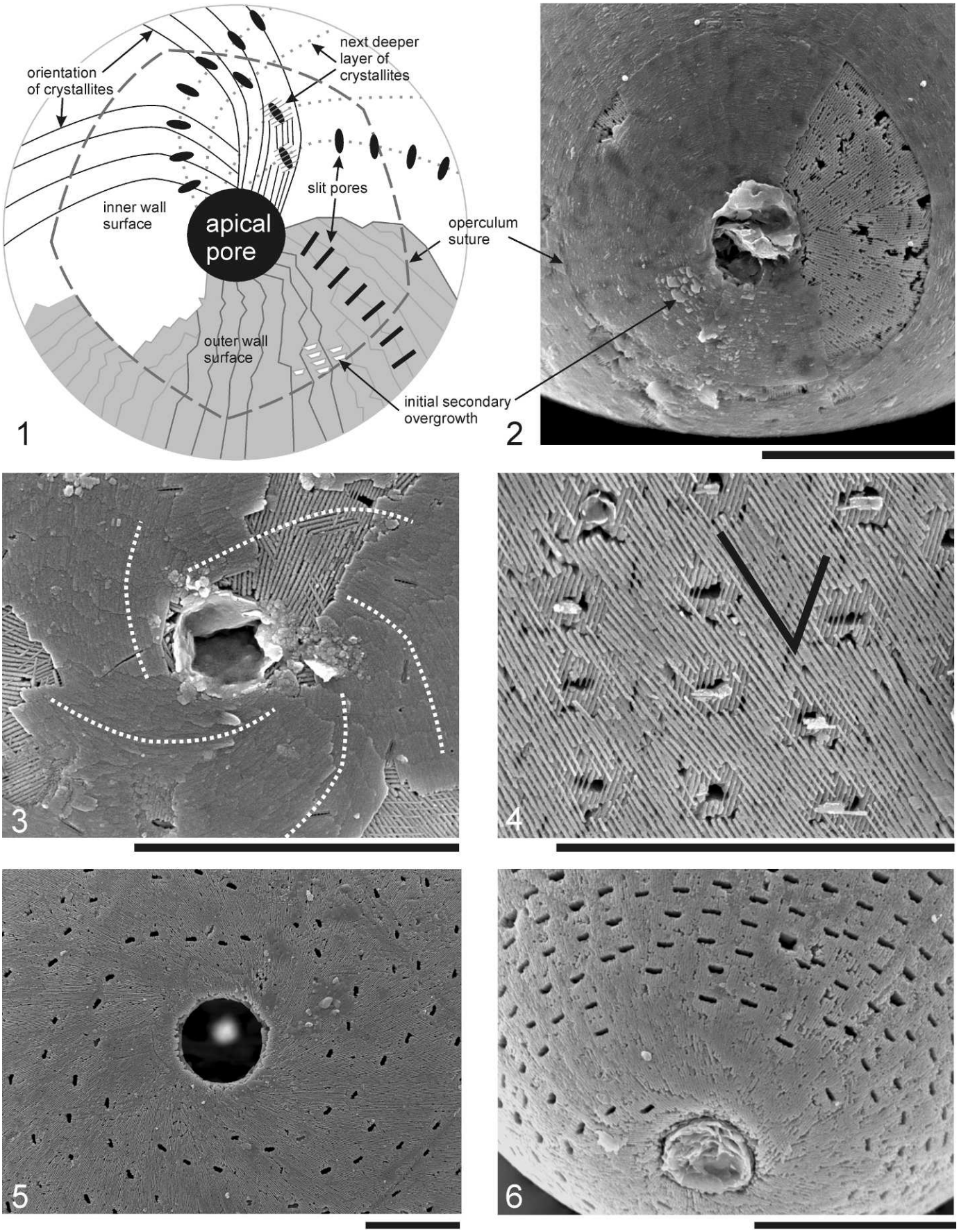

https://doi.org/10.1666/12-121 Published online by Cambridge University Press

a crypto-crystalline architecture with a preferred cleavage plane, or 2) the whole cyst represents a heavily recrystallized single-crystal shell. The latter explanation was suggested for similarly preserved material from the upper Albian Kirchrode 1/91 research drill hole (Keupp and Kienel, 1994). However, such an interpretation is inconsistent with our observations of small cobble-like crystal ends on the inner surface, preserved pores, and lack of overgrowth (Figs. 6.5, 10.2). Therefore, we suggest that a primary, crypto-crystalline architecture is the cause of the compact wall appearance. CL-spectral analysis (J. E. Wendler et al., 2012) further indicates that diagenetic alteration is absent because of a blue luminescence, which is characteristic of primary biomineralized calcite. The micro-crystallites are layered to form a concentric lamellar wall. Multi-layering is illustrated in Figure 10.5 and 10.6. This early phase of recrystallization can be present along with the pristine wall-architecture within one and the same specimen. Apparently, the initial recrystallization brings out the original multiple-layered architecture of the inner wall, revealing four to six individual layers that are distinguishable in this example. In more advanced recrystallized stages (Fig. 10.8, 10.10) the inner wall crystals are columnar shaped with pyramidal tips that are elongated towards the inner cyst (compare also to Villain, 1992, pl. 1, fig. 2), and ultimately the layering disappears completely. Slit pores are finally in-filled with the growing calcite and so disappear with both recrystallization and overgrowth.

Shell etching is frequently present as another expression of earliest diagenetic transformations (Fig. 11). Pithonellid microfossils with similar characteristics that have been described from Kenya were interpreted as the product of incomplete mineralization at a juvenile ontogenetic stage (Villain, 1992). Signs of dissolution are mainly observed on the outer surface of the inner wall in cysts lacking the outer wall. The parallel, longitudinal rows of pores that characterize the inner-wall surface (Fig. 11.2) are initially enhanced by etching (Figs. 11.4, 12.2). Strong etching leads to a needle-like appearance of the crystallite ends (Fig. 11.7, 11.8). Various stages of preservation can occur on the same specimen (Fig. 11.1, 11.3). In some cases the surroundings of the slit pores with denser biomineralization is exposed by etching, resulting in a columnar appearance and resembling hollow tubes (Fig. 11.6; see also Figs. 4.2 and 8.12). Such microstructures were described previously and used to characterize the pithonellid genus and species *Wallia melloi* (Keupp, 1990). The fact that we can show such hollow tube phenomena to be common in *P. ovalis* and *P. sphaerica* calls into question the validity of the genus *Wallia* and consolidates earlier notions of possible pores in *P. sphaerica* (Janofske, 1992; Keupp and Kienel, 1994).

All primary structures and particularly the pore system are ultimately hidden by strong diagenetic overgrowth (Fig. 12). This overgrowth initially may enhance primary structures such as the operculum suture (Fig. 12.4, 12.6) and the shingle-pattern of the outer wall (Fig. 13.1, 13.2). Initial overgrowth clearly follows these shingle rows (Fig. 13.4, 13.6) and reflects the spiral pattern around the poles even in heavily overgrown specimens (Fig. 12.1, 12.3, 12.5). Overgrowth has only been observed on the outer wall (Figs. 12.1, 13.3, 13.5, 13.6). On some strongly overgrown cysts the presence of the outer wall can be detected between the cement crystals (Fig. 12.3 detail). The slit pores might still be visible in moderately overgrown specimens (Fig. 13.5, 13.9). Overgrowth and etching might be found on the same specimen (Fig. 13.7).

Stable isotopes and wall-chemistry.—The long stratigraphic range of many calcareous dinoflagellate and pithonellid species could allow for construction of long single-species isotopic records, which is advantageous over the much shorter ranging planktonic foraminifera because of the uncertainty that is introduced through different vital effects when combining different species in a record. Understanding the ecology and isotopic signal of these fossils is therefore desirable and, hence, considered here in some detail.

An oxygen isotope value from a sample of cement-free *P. sphaerica* (pilot study on middle Turonian large specimens from TDP Site 31) is –4.3‰ (VPDB) and the stable carbon isotope value is +3.6‰ (VPDB) (Fig. 14A). Although pithonellids are abundant in the studied samples, the large difference in $\delta^{13}C$ between *P. sphaerica* and the bulk sediments indicates that the cysts do not contribute significantly to the carbonate content in the Tanzanian material. The preliminary values found here show a similar pattern as Campanian *P. sphaerica* from a chalk section in Lägerdorf, Germany (H. Willems, personal commun., 2012). Comparison with other species is limited because, so far, stable isotope data only exist for one living species, *Thoracosphaera heimii*, and for two Cretaceous microfossils presumed to be calcareous dinoflagellate cysts (but lacking tabulation): *Orthopithonella globosa* and *Pirumella krasheninnikovii*. The latter were reported to have $\delta^{18}O$ values comparable to co-occurring planktic foraminifera and with significantly lighter $\delta^{13}C$ values, similar to many coccolith species (Friedrich and Meier, 2003, 2006). The oxygen isotope value of *P. sphaerica* also indicates surface water temperatures in the same range of values from co-occurring trochospiral planktic foraminifera, but the $\delta^{13}C$ value is very high

→

FIGURE *10*—Recrystallization path from pristine towards overgrown preservation stages of *Pithonella ovalis*. *1,* pristine specimen showing an unaltered outer wall consisting of shingle-like plates creating a pole-to-pole oriented parallel and wavy striation, scale=10 μm; *2, 3,* details of the pristine wall showing the homogenous, micro-crystalline structure of the inner wall, thin veneer-like outer wall and smooth inner surface, scale=5 μm; *4*, specimen with scattered initial overgrowth of prismatic crystals on the outer wall; note partially split-off outer wall showing inner wall surface lacking overgrowth, scale=10 μm; *5,* apical latitudinal section showing laminated structure revealed by initial recrystallization, scale=5 μm; *6,* specimen with well-defined multiple-layered wall architecture, scale=5 μm; *7,* recrystallized cyst with strong overgrowth of prismatic surface crystals, pores are barely visible, scale=10 μm; *8,* inner-wall crystals in typical re-crystallized "bone-shaped" form suggesting only one wall-layer, scale=5 μm; *9,* overgrown "end-member" showing idiomorphic prismatic surface crystals arranged in parallel rows that form the typical parquet surface pattern after diagenetic recrystallization, scale=10 μm; *10,* wall cross-section showing the blocky prismatic secondary crystals within the wall and on the cyst interior surface, scale=5 μm.

→

FIGURE *11*—Diagenetic dissolution structures. *1–7*, *Pithonella ovalis*: *1,* cyst surface showing well-preserved outer wall and partial surface etching; *2,* well-preserved inner wall surface revealing distinctive slit-pore pattern; *3,* well-preserved outer wall with spots of initial overgrowth and areas of dissolution; *4,* strongly etched inner wall and missing outer wall; *5,* partial dissolution (left-hand side) on cyst interior surface enhances pore architecture with prominent rims reflecting the dense pore surroundings; *6,* strongly etched inner wall surface where denser pore surroundings are revealed and lead to tube-like appearance, outer wall is partly preserved (upper right); *7,* oblique wall section of etched specimen showing the superficial nature of etching; note that the homogeneous, crypto-crystalline microstructure is still preserved (broken part in upper left); *8, Pithonella sphaerica*, broken specimen with needle-like appearance on inner cyst surface due to strong dissolution. All scales=10 μm.

https://doi.org/10.1666/12-121 Published online by Cambridge University Press

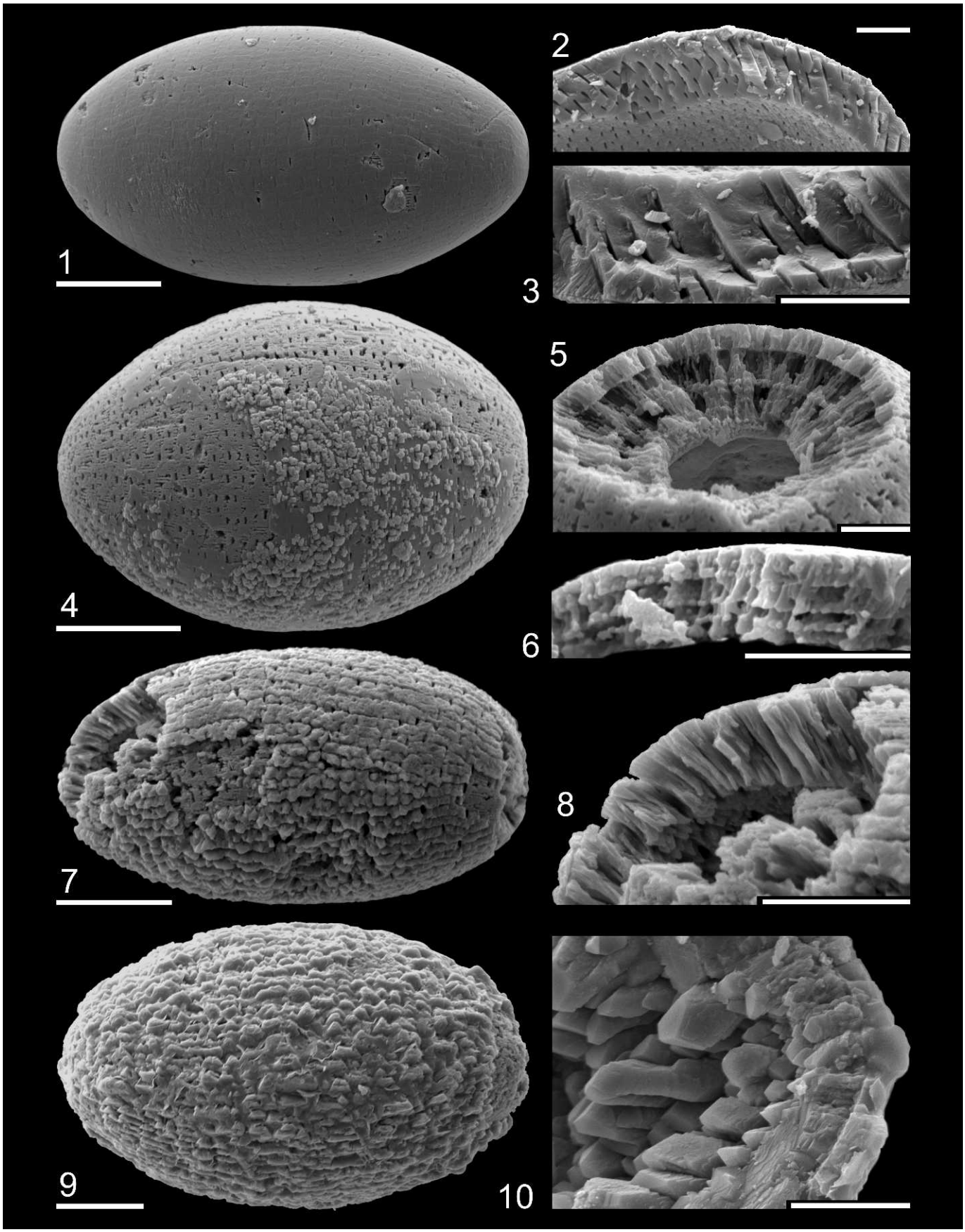

https://doi.org/10.1666/12-121 Published online by Cambridge University Press

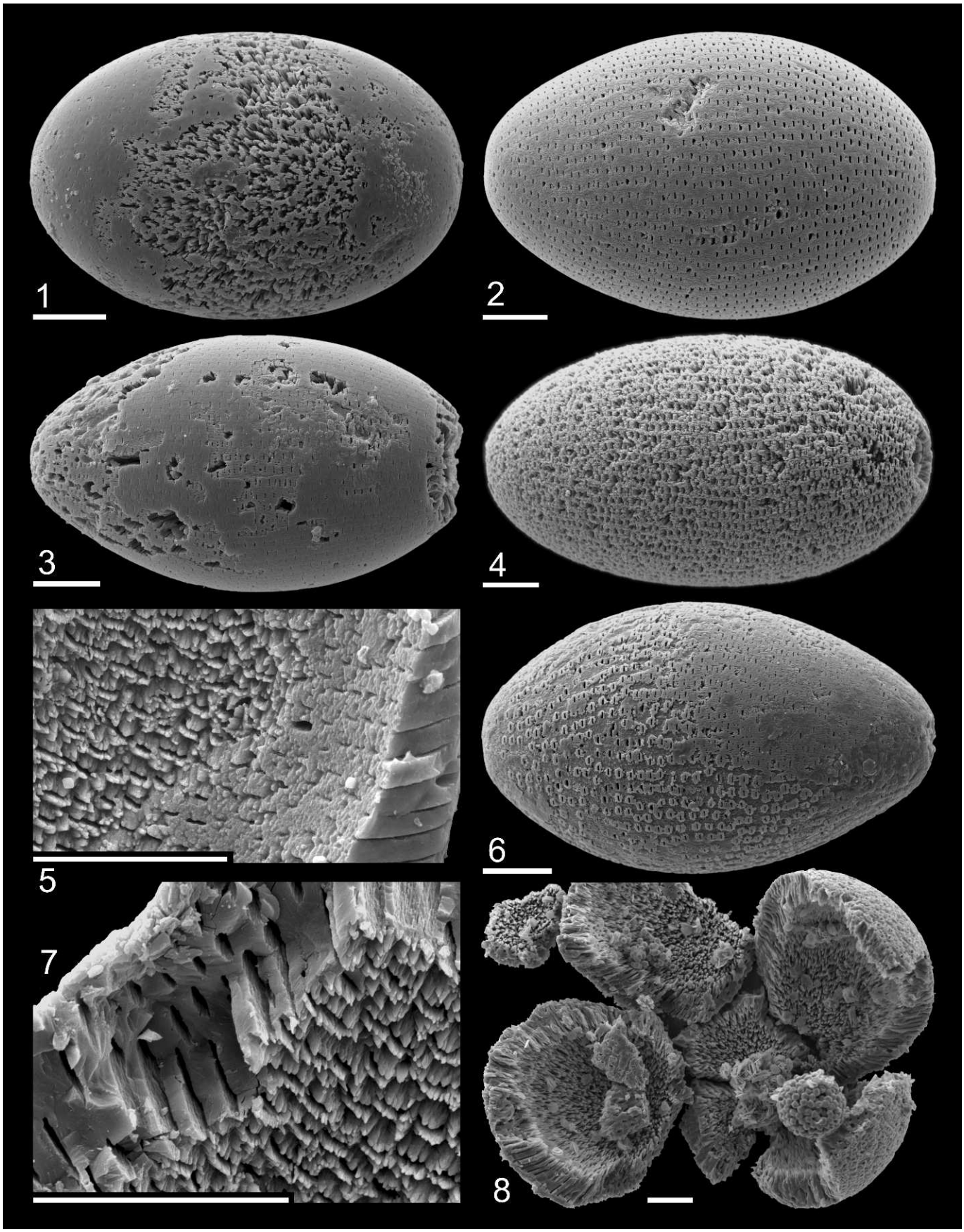

https://doi.org/10.1666/12-121 Published online by Cambridge University Press

(Fig. 14A), unlike the very low values reported from the two other Cretaceous species (Friedrich and Meier, 2003; 2006) and from *T. heimii* which has depleted $\delta^{13}C$ values relative to isotopic equilibrium (Kohn and Zonneveld, 2010; Zonneveld, 2004; Zonneveld et al., 2007).

The most effective mechanism to increase $\delta^{13}C$ in a shell is through selective removal of ^{12}C from the calcification site through photosynthesis, as in photosymbiotic foraminifera (e.g., Norris, 1998). In this case, the sites of photosynthesis and calcification are separated, which leads to ^{12}C-enrichment in the organic material of the symbiont and to ^{12}C-depletion in the test of the host due to the ^{12}C-depleted microenvironment created by the symbionts. The situation is slightly different in a unicellular, phototrophic and calcifying organism, where both processes occur within one cell. Whether or not the ^{12}C-depletion of the medium through photosynthetic build-up of organic material affects the $\delta^{13}C$ of the calcite test depends on the carbon pool that is used for calcification. While all modern calcareous dinoflagellates are phototrophic, *T. heimii* and the two discussed Cretaceous species have comparably low $\delta^{13}C$ values, thus pointing at usage of a $\delta^{12}C$-enriched carbon pool for calcification, possibly influenced by isotopically light CO_2 from respiration. If *P. sphaerica* was phototrophic the species must have used a different biomineralization pathway without using ^{12}C-enriched metabolic CO_2 for calcification. Instead, photosynthetic activity could have created a ^{12}C-depleted internal carbon pool that was also used for calcification.

Although *Pithonella* has some similarity to *T. heimii* with respect to 1) its high abundance; 2) the relatively small size and round shape of the opening; and 3) the presence of numerous pores, they clearly differ in their wall texture and isotopic signature. Differences in wall texture result from different mechanisms of biomineralization, similar to the difference between radial and porcellaneous foraminifera (Weiner and Addadi, 2011), which could also cause different isotopic fractionation. Alternatively, a difference in life strategy or metabolism might be responsible for the different isotopic signature between the two species. It should be noted that the small (~10–20 μm), frequently formed vegetative cysts of *T. heimii* are not necessarily comparable to those of the larger (~30 μm) resting cysts of most other modern dinoflagellate species that are formed less frequently during sexual reproduction, but for which no isotope data are available to date. More stable isotope data from calcareous cysts of modern and fossil dinoflagellates are needed to reveal whether or not there is a large inter-specific variability in isotopic signature as has been described for different coccolith species (Ziveri et al., 2003). Similar to *Pithonella*, enriched $\delta^{13}C$ values of 4–5‰ (Wefer, 1985) were measured in the dasycladacean species *Acetabularia crenulata*, but a number of other arguments speak against an affiliation of pithonellids with dasycladaceans, as discussed below.

Microprobe measurements (Fig. 14B) reveal significantly higher Mg-content in *Pithonella* calcite (1.7–2.2 wt.% MgO) compared to foraminiferal calcite (0.1–0.5 wt.% MgO). Comparably Mg-rich calcite chemistry is also reported from recent calcareous dinoflagellates (Ho et al., 2003). The Mg content indicates two important aspects: 1) the $MgCO_3$ is iso-structural in the calcite microstructure, so the high Mg content of the pristine shells proves that *Pithonella* could not have been originally aragonitic and 2) the incorporation of Mg in the calcite lattice causes calcite to be unstable, and tending to stabilize to low-Mg calcite. Importantly, this may explain the susceptibility to recrystallization and the global rarity of well-preserved pithonellid microfossils.

Taxonomic affinity.—An affiliation of pithonellid calcitarchs with the Thoracosphaeraceae has been previously questioned (Elbrächter et al., 2008; Streng et al., 2004; Versteegh et al., 2009). In searching for plausible alternative affinities, there are similarities between the operculum area of *Pithonella* and the cysts of the dasycladaceen alga *Chalmasia antillana* Solms-Laubach, 1895 (previously "*Acetabularia*" *antillana*). *Chalmasia antillana* forms spherical, calcareous cysts with an operculum (Marszalek, 1975). With a size of 140 to 185 μm diameter, these cysts are on average larger than *Pithonella*, which is dominantly 20–80 μm and only rarely reaches diameters up to 180 μm. However, the description of the operculum by Marszalek compares well with our observations except for the central pore: "The operculum is a convex disc 40 μm in diameter and 10 to 25 μm thick. The circular perimeter is slightly tapered towards the interior of the calcisphere. The circular outline of the operculum is visible on the surface of the intact calcisphere in the SEM; in transmitted light the disc absorbs more light than does the remainder of the cyst and appears as a darker, circular area." Despite this similarity in optical appearance, *Acetabularia*, like all other dasycladacean algae, has a considerably different environmental distribution than *Pithonella*; Dasycladaceae are restricted to shallow coastal environments of only a few meters water depth and they require attachment, whereas all species of *Pithonella* were common in outer shelf to upper slope environments (Bein and Reiss, 1976; Dali-Ressot, 1987; Dias-Brito, 2000; Villain, 1981; J. E. Wendler et al., 2002a; Zügel, 1994). Furthermore, there are no reports of coastal Cretaceous deposits in which *Pithonella* cysts are found attached to dasyclad remains, which should be expected given their high abundances

→

FIGURE *12*—Disguise and enhancement of primary structures through diagenesis in *Pithonella sphaerica*, oblique-lateral views with apical poles oriented to the left except in *4* and *6* that show apical views. *1, 3, 5,* increasing overgrowth with secondary calcite, note that the spiral pattern is reflected in the overgrowth in all three stages, early overgrowth is seen only on patches of the outer wall (*1*), the outer wall can be well preserved underneath strong overgrowth (detail in *3*); *2,* etched inner wall surface showing the typical striation visible in light-optical imaging but invisible in un-etched surfaces; *4, 6,* apical view of operculum with apical pore, the operculum suture is enhanced by thin (*4*) or intermediate (*6*) overgrowth. All scales=10 μm.

→

FIGURE *13*—Influence of overgrowth on primary traits in *Pithonella ovalis* (except *3* showing *Pithonella sphaerica*). *1, 2,* shingle-like pattern of the outer wall enhanced by initial recrystallization, antapical pole (*1*) and apical pole (*2*), scale=5 μm; *3,* strong overgrowth only on outer wall (arrow), note former pores as inter-crystal holes, scale=5 μm; *4,* early patch-like overgrowth following the shingle-like pattern of the outer wall and forming the typical parquet pattern known from pithonellids, scale=5 μm; *5,* moderate overgrowth preserving hints of the pores, outer wall and overgrowth are missing on the right-hand side where inner wall and pores are well preserved, scale=10 μm; *6,* parquet-like striation of overgrowth reflecting the rows of the shingle-like pattern of the outer wall (see *1* and *2*), scale=10 μm; *7,* longitudinal cross-section showing thick overgrowth (arrow in enlarged view) co-occurring with dissolution on the cysts inside (arrow in overview), pores and cryptocrystalline structure of the inner wall are well preserved, scale=20 μm; *8,* patches of outer wall with overgrowth and inner wall without overgrowth, scale=10 μm; *9,* disappearance of slit-pores with overgrowth, scale=10 μm.

https://doi.org/10.1666/12-121 Published online by Cambridge University Press

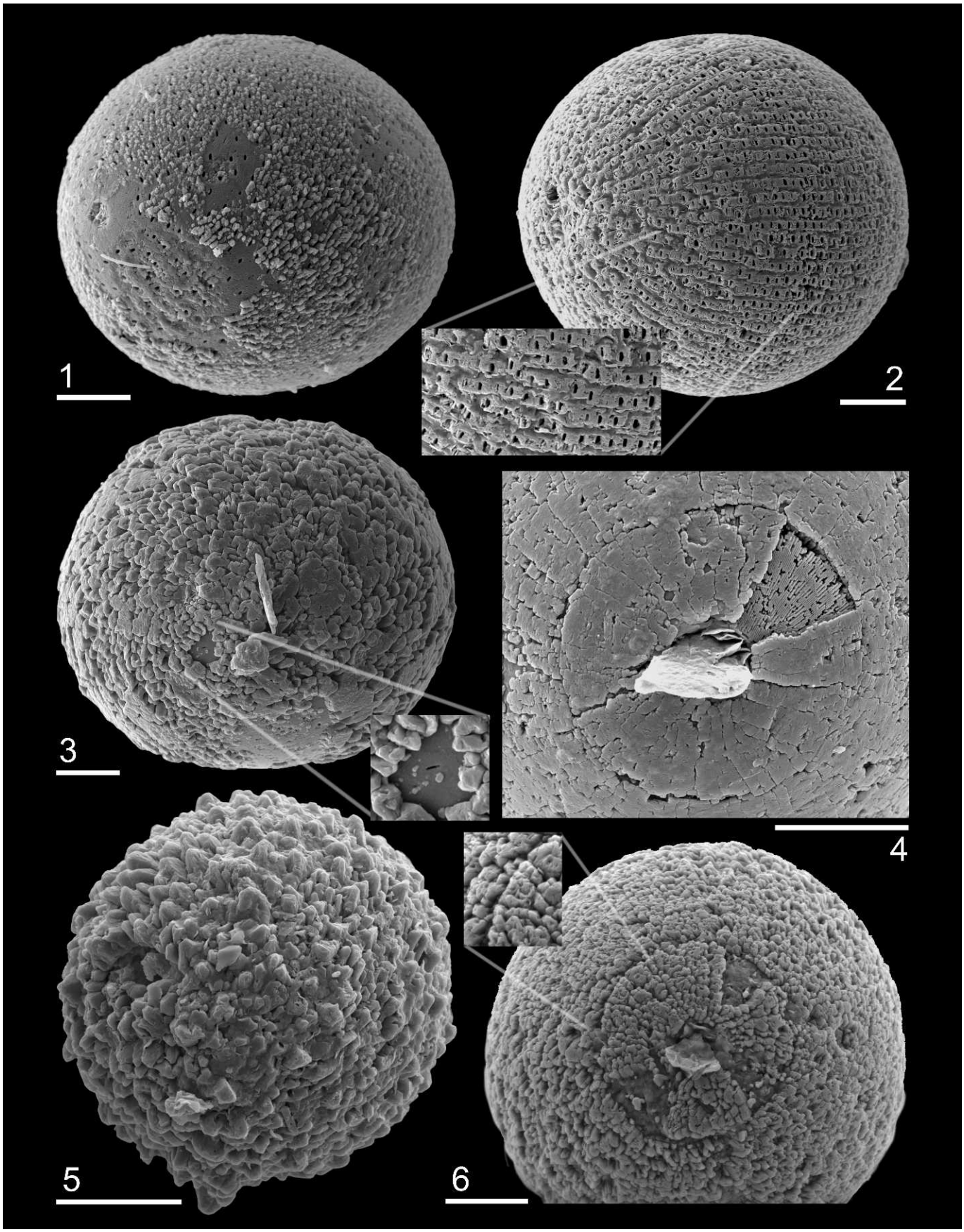

https://doi.org/10.1666/12-121 Published online by Cambridge University Press

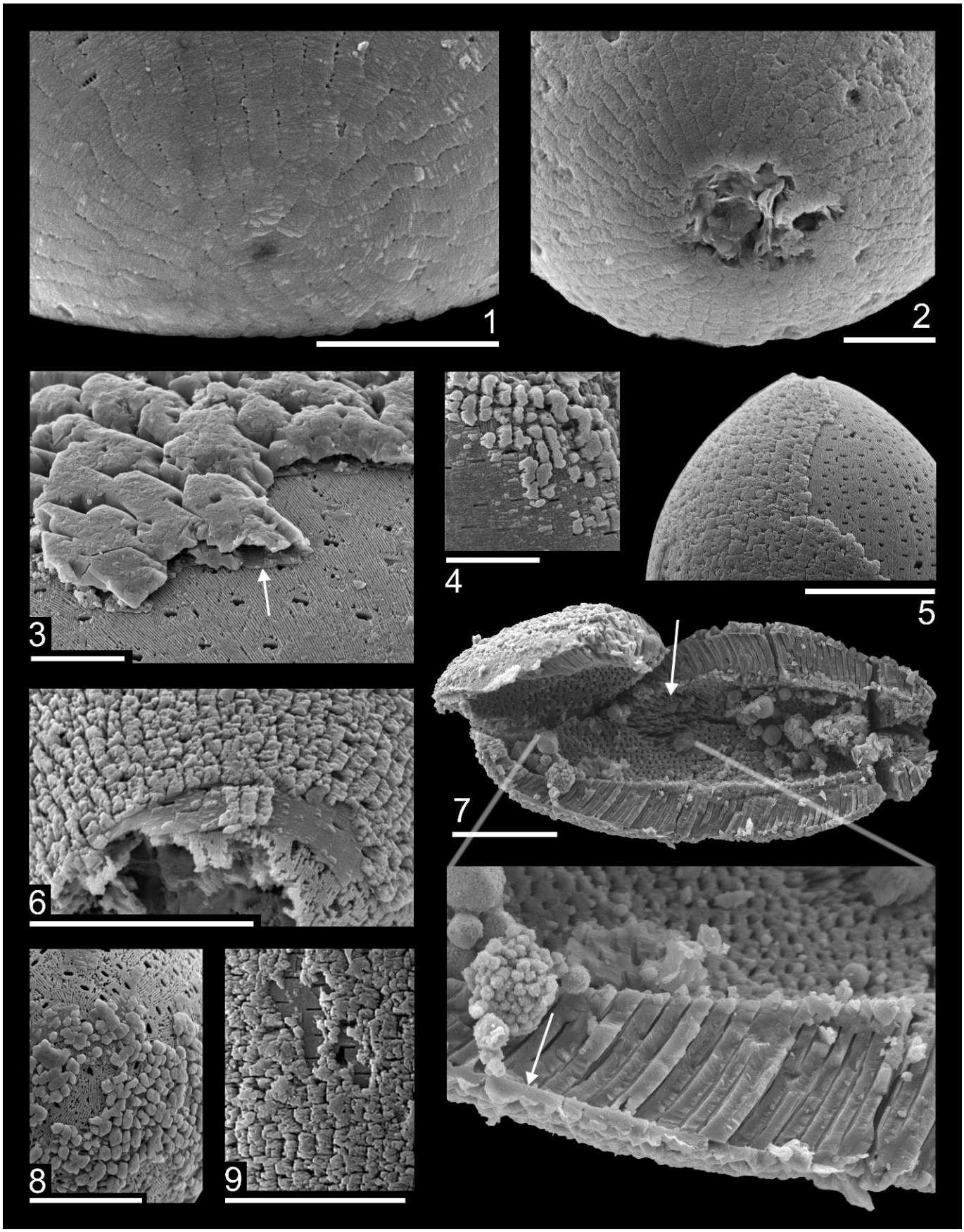

https://doi.org/10.1666/12-121 Published online by Cambridge University Press

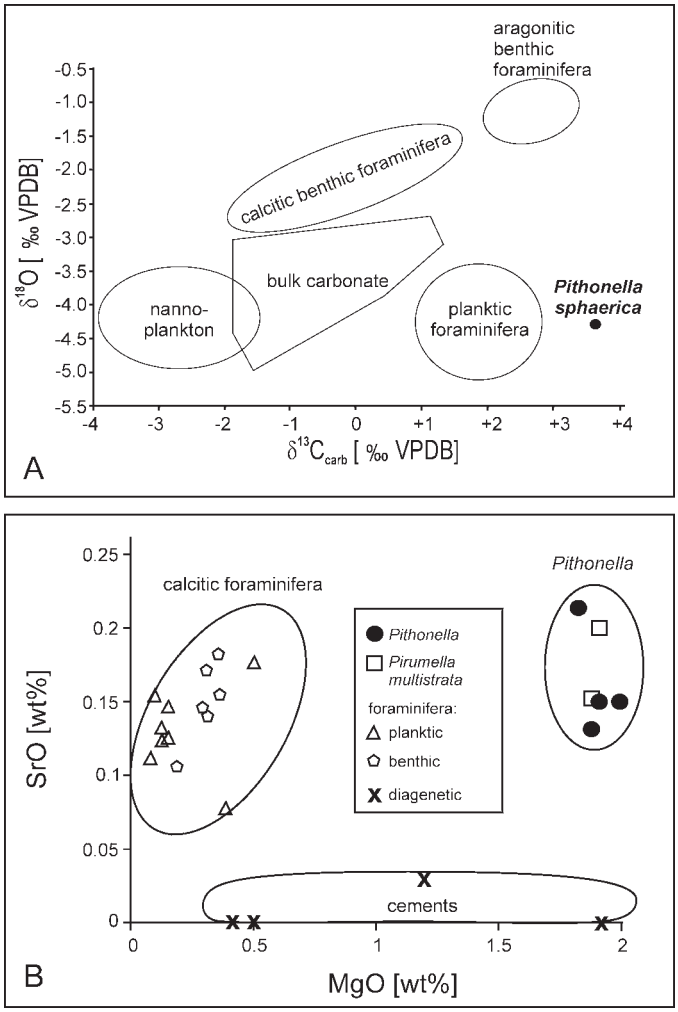

FIGURE 14—Carbonate geochemistry of *Pithonella*. *A,* cross-plot $\delta^{13}C$ versus $\delta^{18}O$ for the early Turonian of TDP Site 31 showing a measurement obtained from large *Pithonella sphaerica* in relation to isotope value ranges for co-occurring benthic and planktonic foraminifera and bulk carbonate (I. Wendler et al., 2013), and known ranges for calcareous nannofossils, similar oxygen isotope values of *Pithonella* and planktic foraminifera indicate a surface water habitat for *Pithonella*; *B,* cross-plot of SrO versus MgO for *Pithonella* and other common carbonate particles in the TDP material. Note the distinctly elevated MgO content in *Pithonella* and *Pirumella multistrata*, making these shells prone to diagenetic alteration.

and widespread distribution. Instead, *Pithonella* cysts appear to decrease in abundance and finally disappear shoreward (Zügel, 1994). In addition, modern *Acetabularia* "calcispheres" do not survive transport over any appreciable distance and are therefore not found beyond inner shelf depths (Marszalek, 1975). Most importantly, the $\delta^{18}O$ of *Pithonella* indicates a cyst formation in surface waters but the paleo-bathymetric position of the investigated section was on the upper slope. Therefore, sea floor substrate for attachment required by a dasyclad life strategy was not available in the photic zone. A further important difference between *Pithonella* and *Acetabularia* is that the latter produces aragonitic cysts while *Pithonella* formed a calcitic cyst (see above). Based on these differences we conclude that dasycladacean algae, as we know them from modern times, are unlikely to have produced *P. sphaerica* and *P. ovalis*. Other interpretations of the origin of the calcisphere species *P. sphaerica* and *P. ovalis* suggested that they might be benthic foraminifera (Colom, 1955). However, presence of an operculum and the biomineralization pattern (see below) of *Pithonella* rule out any association with foraminifera.

The presence of an antapical pore in pithonellids could, with the current state of knowledge, be taken as an argument against their possible affinity with the dinoflagellates because antapical pores have not yet been described for these latter organisms. On the other hand, it could be speculated that an additional opening for pressure regulation would promote the hatching process. Alternatively, the presence of two openings evokes comparison with the mouth/anus duality in animals. Some thecameboians with pores in either test pole are known, but these organisms are characteristic for terrestrial freshwater (and rarely brackish) habitats and typically form non-calcitic tests, except for few species with large calcite plates that have nothing in common with the pithonellid wall architecture.

Affiliation of pithonellid calcitarchs with the Thoracosphaeraceae critically depends on two aspects: 1) the biomineralization, as it is reflected in pristine material, must be comparable to biomineralization models of known Thoracosphaeraceae and 2) the operculum and opening must be comparable to opercula and archeopyles of known dinoflagellates. Regarding the first criterion, our observations (Fig. 15) strongly support the model of biomineralization in pithonellids established by Keupp and Kienel (1994), which corresponds to biomineralization in recent calcareous dinoflagellates (Gao et al., 1989). In those models for calcareous dinoflagellate cyst biomineralization, the principle crystallization areas are determined by an organic skeleton: an inner organic cell membrane lines the cyst inside, an intermediate organic wall separates inner from outer wall, an outer organic membrane surrounds the cyst, and a pore system connects all organic walls. The outer calcitic wall forms between the intermediate and outer organic membranes and the inner calcitic wall forms between the inner and intermediate membrane and pore linings (Fig. 15.1). We interpret the slit-pores of *Pithonella* as elements of an organic skeleton that primarily constituted the cyst body and a biomineralization space. The Tanzanian material reveals evidence of all three membranes and possible organic remains (Fig. 15.2, 15.3, 15.4) comparable to finds within cultured recent calcareous dinoflagellates (Fig. 15.5, 15.6) were observed. Furthermore, the ply-like partly interwoven submicron-scale wall-fabrics of pithonellids are comparable to that seen in certain living dinoflagellates that form calcareous cysts, specifically *Leonella granifera* (Wendler and Bown, 2013).

Concerning the second aspect, the architecture of the opercula and the apical pore merits further discussion of two potential interpretations. First, the apical pore on *P. sphaerica* could be interpreted to reflect the apical pore complex of motile cells (Fig. 1.1a) as is observed on cysts of the modern species *Calciodinellum operosum* (Kerntopf, 1997; see also Fig. 1.6, 1.7). While the latter species has a larger compound operculum that also includes the 1a, 2a and 3a plates of the peridinialean tabulation (Fig. 1.1a and 1.6), the operculum of *Pithonella* could comprise only the 2′, 3′, and 4′ plates (Fig. 1.1 and 1.7). The three plates would form the observed sub-angular shape of the operculum (Figs. 3.1a, 3.2c, 9.1) with a nook on the side that is in contact with the 1′ plate (e.g., upper left in Fig. 3.1a), thus representing a simple operculum providing a polyplacoid archeopyle of type (3A) according to the classification of archeopyle types (Evitt, 1967; Evitt, 1985). This interpretation could also explain the opercula shapes of *P. lamellata* and *Pirumella multistrata* with their central pores (Fig. 4.6, 4.7). However this would imply relatively small plates for these species.

An alternative interpretation is that the entire sub-angular operculum might represent a 3′ plate (type A). In this case the apical pore would be located within the 3′ plate. Such a feature

https://doi.org/10.1666/12-121 Published online by Cambridge University Press

has not been previously reported for calcareous dinoflagellate cysts. Our revision of multiple specimens of cultured *Leonella granifera* and of the literature data (discussed above) revealed the presence of a knob with a central depression within the operculum whose corresponding archeopyle has been reported to be of type A (Streng et al., 2004), possibly because of its rather small diameter relative to the cyst size. However, in the original diagnosis of the species (and genus) it is stated that: "The small operculum is circular and includes apical plates" (Janofske and Karwath, 2000). The usage of plural here indicates that these authors suspected that multiple plates are present in the operculum of *L. granifera* despite its small size. It is interesting to note that the apical pore of the motile cell of *L. granifera* was described as circular with an elevated rim (Janofske and Karwath, 2000), much like the feature that can be observed in the middle of the operculum in cysts of *L. granifera* (Fig. 1.5). Given the similarity between *L. granifera* and *Pithonella* in the characteristics of the cyst body (lack of tabulation), of the operculum (round to sub-angular and rather small) and of the fine, grid-like architecture of the cyst wall (compare Fig. 15.6b with Figs. 10.6 and 16.2c), and their analogue to the reflected apical pore in the middle between the 2′, 3′, and 4′ plates in *C. operosum*, it appears plausible that *L. granifera* and *Pithonella* both could have a type (3A) archeopyle, as discussed in the previous paragraph.

The slight deviation in crystal inclination of the operculum relative to the cyst body suggests that the whole area is segregated for the purpose of shell break-up (Figs. 3.1, 4.2, 4.5). Interestingly, for some dinoflagellate cysts, even though a suture may mark the outline of the operculum, this structure isn't finally used for hatching (Versteegh, 1993). Instead, Versteegh notes that this cyst part features a different shell architecture/density or a smaller thickness such that a portion of it can be cracked or dissolved during hatching, leaving an irregular smaller opening. The apical pore of *Pithonella* could be interpreted in a similar manner. On the other hand, we frequently found *P. lamellata* and *P. atopa* with openings that resulted from detaching the opercula (Figs. 4.6, 16), while these opercula also feature a central pore (Fig. 4.6). Due to the mentioned ambiguities regarding detachment, it remains possible that the opercula of *P. sphaerica* and *P. ovalis* did not have a cyst-opening function. In summary, the combination of presence of an operculum similar to opercula of known calcareous dinoflagellates, a biomineralization pattern comparable to Thoracosphaeraceae, calcitic cyst chemistry, and a habitat extending to the outer shelf/upper slope lend strong support in favor of an association of the genus *Pithonella* with open-marine cyst-forming organisms, including the dinoflagellates. Nevertheless, the lack of unequivocal, complete peridinoid tabulation still remains a limitation for the affiliation of *Pithonella* with the dinoflagellates. A summary of the morphological features of pithonellids that are used to argue for or against their dinoflagellate affiliation and some alternative interpretations are provided in Table 1.

SYSTEMATIC PALEONTOLOGY

Incertae sedis
Group CALCITARCHA Versteegh et al., 2009

Remarks.—The genus *Pithonella* represents calcareous cyst-forming microorganisms (this study) having probable affiliation with dinoflagellates.

Division DINOFLAGELLATA (Bütschli, 1885) Fensome et al., 1993
Subdivision DINOKARYOTA Fensome et al., 1993
Class DINOPHYCEAE Pascher, 1914
Subclass PERIDINIPHYCIDAE Fensome et al., 1993
Order PERIDINIALES Haeckel, 1894
Suborder PERIDINIINEAE Autonym
Family THORACOSPHAERACEAE Schiller, 1930

Remarks.—Keupp (1987) introduced the Pithonelloideae as a subfamily of the family Calciodinellaceae Deflandre, 1947: "Dinoflagellate cysts with a single or double calcitic wall. Outer wall surface crystallites, and often also inner wall surface crystals are uniformly obliquely oriented in a regular parquet-pattern in straight or spiraling rows" Keupp (1987, p. 39). This subfamily is not generally accepted and is not mentioned in the nomenclatural synopsis of Elbrächter et al. (2008) who re-established the family Thoracosphaeraceae thereby also replacing for calcareous dinoflagellates the assignment with the family Peridiniaceae Ehrenberg 1831 and the subfamily Calciodinelloideae Fensome et al., 1993.

Genus PITHONELLA Lorenz, 1902

1902 *Pithonella* LORENZ, p. 46.
1941 *Cadosinella* VOGLER, p. 282.
1956 *Calcisphaerula* BONET, p. 443, pl. 24.
1964 "*Palinosphaera*" VOIGT AND HÄNTZSCHEL, p. 538 [nom. illeg.]
1964 *Pithonella* Lorenz, 1902 emend. BIGNOT AND LEZAUD, p. 140.
1967 "*Palinosphaera*" REINSCH *in* LOCKER, p. 852 [nom. illeg.]
1974 *Andriella* BOLLI, p. 845.
1977 *Pithonella* Lorenz, 1902 emend. VILLAIN, p. 144.
1987 *Pithonella* Lorenz, 1902 emend. KEUPP, p. 39.
1990 *Wallia* KEUPP, p. 49.
1994 *Pithonella* Lorenz, 1902 emend. ZÜGEL, p. 24.

Type.—The neotype of *Pithonella ovalis* (Kaufmann *in* Heer, 1865) Wendler and Wendler, herein, Figure 17.

Included species.—*Pithonella ovalis* (Kaufmann *in* Heer, 1865) Wendler and Wendler, this study (=*Lagena ovalis*), *P. sphaerica* (Kaufmann *in* Heer, 1865) Villain 1977=*Lagena sphaerica*) , *P. multicava* Borza, 1972 (senior synonym of *P. perlonga* Andri, 1972), present in Tanzania (Fig. 18.1), "*P. trejoi*" Bonet, 1956 (name not validly published), present in Tanzania (Fig. 18.2), *P. discoidea* Willems, 1992, present in Tanzania (Fig. 18.5, 18.6), *P. melloi* (Keupp, 1990) Wendler and Wendler, n. comb., *P. cardiiformis* Zügel, 1994, *P. pyramidalis* Willems, 1994 and, *P. diconica* Wendler and Wendler n. sp. (Fig. 18.3, 18.4).

→

FIGURE 15—Biomineralization, comparison with modern calcareous dinoflagellate cysts. *1,* scheme of the organic skeleton formed by the pore system and three membranes which constituted the calcification spaces for the inner and outer wall, Ap=apical pore, Aap=antapical pore; *2,* possible remains of an organic membrane on *Pithonella sphaerica*, oval-shaped holes likely reflect the pore system, scale=5 μm; *3,* longitudinal cross-section of *Pithonella ovalis* showing organic remains of the outer and possibly inner membrane, platy minerals are clay minerals that entered the apical pore, scale=10 μm; *4*, detail of *3* showing spherical organic particle that is similar to those observed in modern dinoflagellate cysts (compare to *6*), scale=5 μm; *5,* detail of wall cross-section from a cyst of cultured *Calciodinellum albatrosianum* (modern calcareous dinoflagellate) showing formation of the calcitic wall crystals between a thick inner membrane and a thin outer membrane, scale=5 μm; *6a,* cracked cyst of cultured *Leonella granifera* (modern calcareous dinoflagellate) showing numerous organic particles (probably starch) inside the inner membrane, scale=5 μm; *6b*, detail of wall cross section showing fine, grid-like architecture and rod-like crystal arrangement.

https://doi.org/10.1666/12-121 Published online by Cambridge University Press

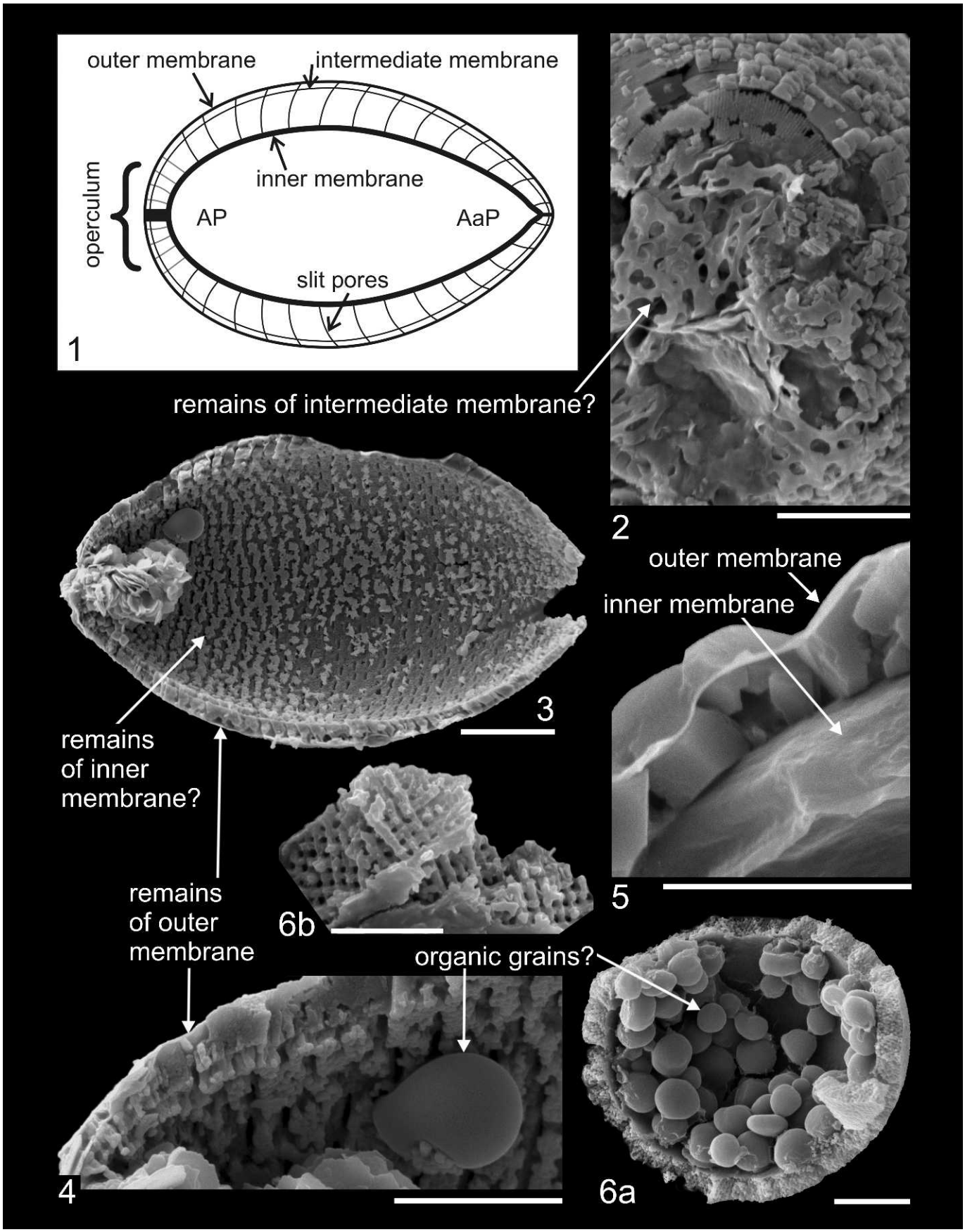

https://doi.org/10.1666/12-121 Published online by Cambridge University Press

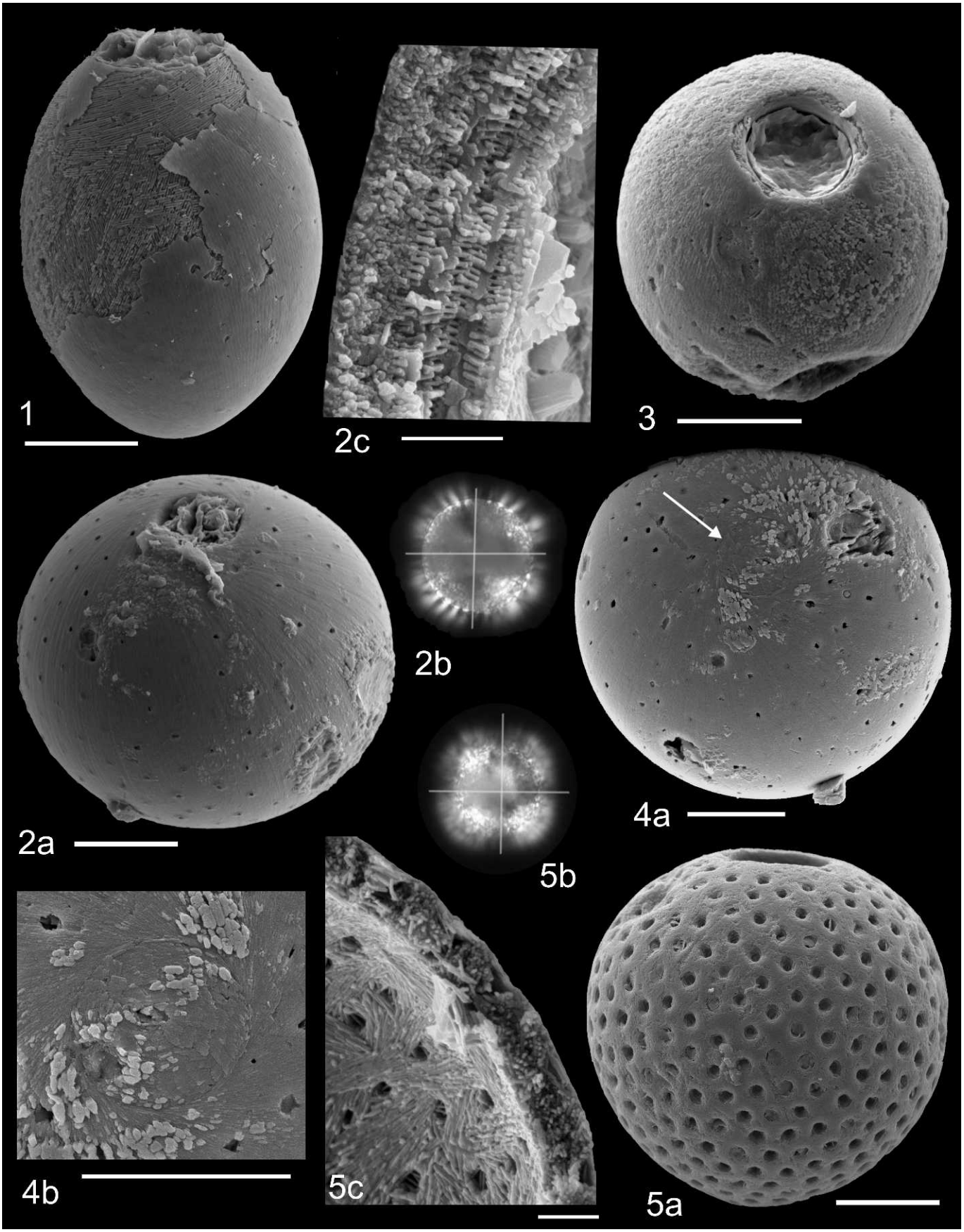

https://doi.org/10.1666/12-121 Published online by Cambridge University Press

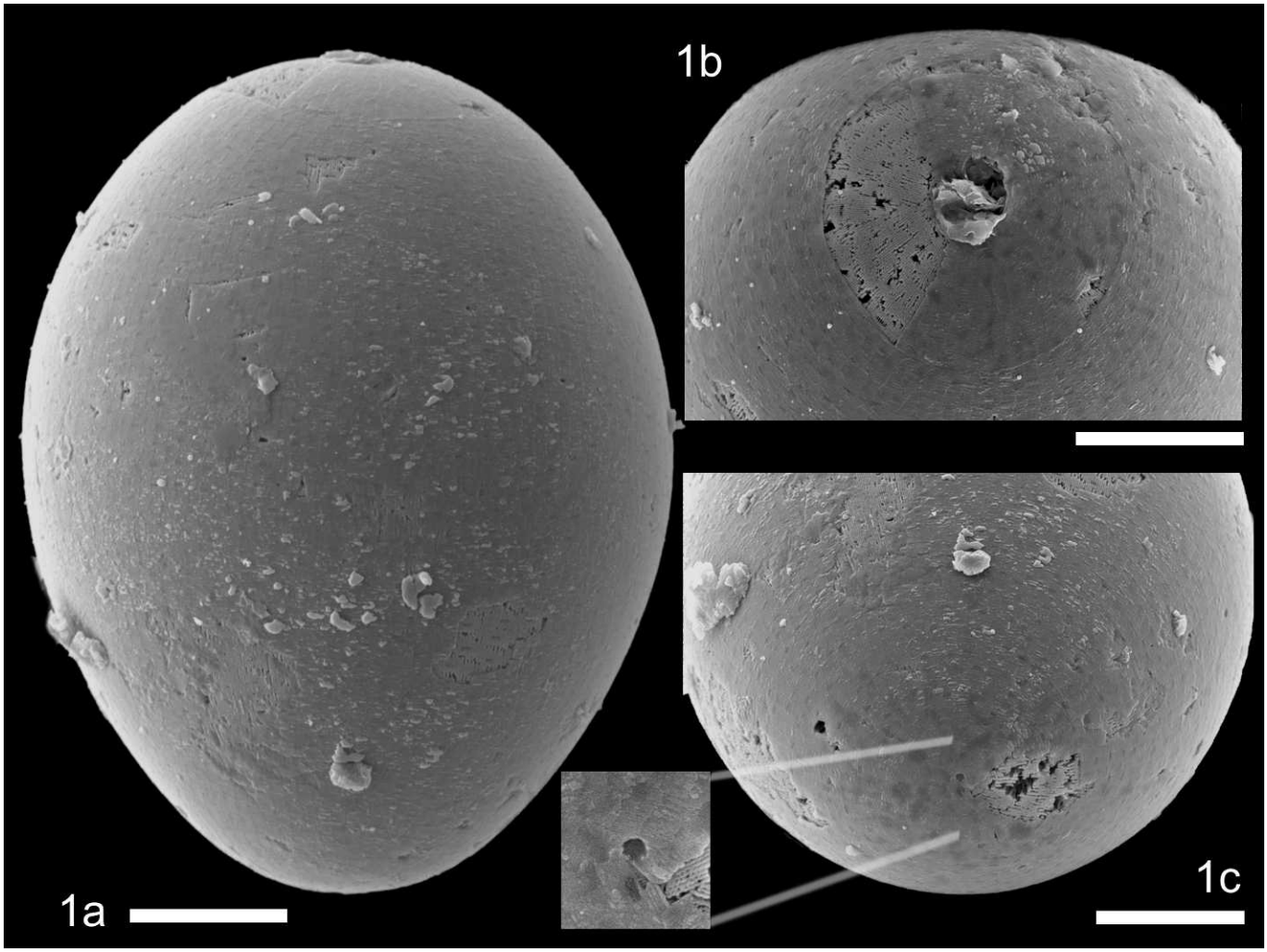

FIGURE 17—Neotype *Pithonella ovalis* specimen TDP22-31-1P_E5 sample # TDP22-31-1 (34–45 cm), scale=10 μm: *1a*, equatorial view; *1b*, apical view showing the operculum; *1c*, antapical view with zoom of antapical pore.

Pithonella atopa Keupp and Kienel, 1994, *P. microgranula* Zügel, 1994, and *P. lamellata* Keupp and Kienel, 1994 (Fig. 16) are pithonellid forms with a granular and lamellar inner wall (Fig. 16.2c, 16.5c) currently included with the genus *Pithonella*. They are composed of uniformly inclined, rod-shaped crystallites (Fig. 16.5c), occur with closed opercula (Fig. 16.4a, 16.4b) and detached opercula (Fig. 16.2a, 16.3, 16.5a), and reveal the typical pithonellid surface pattern (Fig. 16.3, 16.4a, 16.4b) and optical crystallite orientation (Fig. 16.2b, 16.2c, 16.5b). However, they show a significantly different pore system (Fig. 16.2a, 16.4a, 16.4b, 16.5a, 16.5c), operculum-size and shape (compare Fig. 16.4b to Fig. 3), and thus are probably associated with the second pithonellid genus, *Bonetocardiella* Dufour, 1968, emend. Villain, 1975, which shows these traits. A revision of this latter genus and discussion of generic relations within the entire pithonellid group, including the third pithonellid genus *Normandia* Zügel, 1994, is beyond the scope of the present work.

Diagnosis.—Calcareous, spherical, elongated, flattened and pyramidal shells with an apical, circular to sub-angular operculum, and apical and antapical pore. A system of dense

←

FIGURE 16—Additional pithonellid forms present in the Turonian of Tanzania. *1*, *Pithonella* sp. 1, ovoid specimen with detached operculum, similar to *P. ovalis* but lacking the slit-pore system; note the shingle-patterned outer wall and rod-shaped crystallites of several layers of the lamellar inner wall; the well-defined opening is 12 μm in diameter and filled with clay particles; *2a*, *Pithonella lamellata* Keupp and Kienel 1994, slightly flattened specimen with a distinct opening at 8 μm in diameter; pore system consisting of equidistant pores differs from the system of slit pores in the genus *Pithonella* sensu this study; note the spiral surface striation pattern and initial parquet overgrowth; *2b*, specimen in crossed nicols confirming pithonellid crystal orientation; *2c*, wall cross-section illustrating the distinct lamellar wall architecture and the individual rod-like crystallites in uniformly inclined orientation, scale=2 μm; *3*, *Pithonella lamellata* with large opening, and diagenetic overgrowth revealing the distinct pithonellid spiral pattern and parquet-like surface crystal arrangement; *4a*, *Pithonella lamellata* with the operculum still in place (arrow). Note the typical pithonellid surface pattern; *4b*, close-up of the operculum whose crystal orientation differs from the main cyst body, the small, bright crystals represent initial diagenetic surface re-crystallization; *5a*, *Pithonella atopa* Keupp and Kienel 1994 (=*P. microgranula* Zügel), opening diameter is 9 μm, note the distinct pores; *5b*, imaging in crossed nicols confirms pithonellid crystal orientation; *5c*, wall cross section showing the micro-granular wall architecture. All scales=10 μm unless noted otherwise.

https://doi.org/10.1666/12-121 Published online by Cambridge University Press

longitudinal rows of slit-like pores spans the shell wall. Shells are double-walled. The thin, veneer-like outer wall consists of smooth, shingle-like plates in slightly wavy longitudinal rows that can spiral at the poles; early diagenetic recrystallization of surface crystallites to regular parquet-like rows is common. The crypto-crystalline, laminated inner wall shows parallel, rod-shaped crystallites on its distal surface. The sub-micron wall crystallites have a radial, uniformly inclined (pithonellid) crystallographic orientation.

Etymology.—Derived from "pithos" (Greek) for large Greek storage jars of a particular shape occasionally resembled by certain thin-section orientations. This appearance is caused by the widening of the opening towards the inner cavity. A jar-like outer shape in fact occurs in no species of *Pithonella*, but is typical of calpionellids and tintinnids, which are thought to be unrelated to *Pithonella*.

Occurrence.—Upper Barremian–Cretaceous/Paleogene boundary. A comprehensive overview of the stratigraphic and paleogeographic distributions of the species of *Pithonella* is given by Dias-Brito (2000). Paleogeography: Tethyan Realm, between latitudes 40°N and 40°S. Paleoecology: predominantly deeper inner shelf to outer shelf, some occurrences in coastal environments, absent from pelagic environments, thermophilic.

Remarks.—No original diagnosis was provided by Lorenz (1902). Bignot and Lezaud (1964) gave the first diagnosis, based on thin sections: "Small test (< 0.1 mm), spherical or ovoidal. One opening without collar on one pole of the test. Calcareous test-wall, non-perforated, fibrous. The fibers have rectangular orientation relative to the surface at both poles, and oblique orientation in the equatorial region of the test. This orientation causes a non-centered, black axis cross under polarized light (at the oral pole)." Translated from Bignot and Lezaud (1964, p. 140).

Villain (1977) provided the first diagnosis based on isolated specimens: "Test is single-chambered, size varies between 20 and 250 microns, axial symmetry, single opening. The calcareous fibrous test-wall shows, in axial section under polarized light, the phenomenon of a black, marginally-positioned axis cross. In sections perpendicular to the (pole to pole) axis a normal (not excentric) axis cross is seen. The outer morphology is structureless in contrast to the inner test cavity. Good specimens show that the fibers have a regular and ordered arrangement." Translated from Villain (1977, p. 144).

Remarks by Zügel (1994): "Spherical, elongated and flattened cysts lacking further morphologic traits. Two wall architecture types are distinguished: (1) the mostly double-layered inner wall consists of concentric, antapically inclined crystals. Rare exceptions show a granular inner wall with large perforation. (2) The outer wall is constructed of longitudinal rows of prismatic crystals that are latitudinally inclined (anticlockwise in apical view)." (Zügel, 1994, p. 17).

The diagnosis has been emended here. In light of a possible dinoflagellate affinity for *Pithonella*, the operculum can be interpreted as a polyplacoid operculum of type (3A), comprising the 2′, 3′, 4′ plates. Some preservation stages can make the inner wall appear laminated. This is not regarded as ecophenotypical variability as has been suggested previously (Kohring et al., 2005). The genus *Pithonella* has been used earlier for a large number of species (see Keupp, 1981 and references therein), but in its restricted sense contains only those species explicitly assigned here under "included species". Those genera listed as synonyms of *Pithonella* represent monospecific genera whose species have since been synonymized with either of the following four species: *Pithonella sphaerica* (Kaufmann *in* Heer, 1865) Villain, 1977 (=*Calcisphaerula innominata* Bonet, 1956, p. 443, pl. 24="*Palinosphaera sphaerica*" (Kaufmann *in* Heer, 1865) Reinsch *in* Locker, 1967, p. 852 [nom. illeg.]), *Pithonella multicava* Borza, 1972 (=*Cadosinella grasillimoides* Vogler, 1941, p. 282), "*Pithonella trejoi*" Bonet, 1956 (=*Andriella trejoi* Bolli, 1974, p. 845), and *Pithonella melloi* (Keupp, 1990) Wendler and Wendler, n. comb. (basionym=*Wallia melloi* Keupp, 1990, p. 49, pl. 14, fig. 1–12, pl. 15, fig. 1–4). The genus *Wallia*, with its type species *Wallia melloi* Keupp, 1990, was distinguished by a wall architecture showing "hollow crystals". Such tube-like phenomena are associated with the pore system described in the present study. They are present in all species of the genus *Pithonella* as newly diagnosed. Therefore, we place the apically flattened forms of *Wallia* in junior synonymy with *Pithonella* and have transferred the type species of *Wallia* to *Pithonella*. Additional genera to which *Pithonella* (*P. sphaerica*) has been assigned but remain valid for all other species they contain are *Lagena* (*L. sphaerica* Kaufmann *in* Heer, 1865, p. 196), *Stomiosphaera* (*S. sphaerica* Kaufmann *in* Heer, 1865; Bonet 1956, p. 64, pl. 23; Andri, 1972, p. 26), and *Pleurozonaria* (*P. globulus* Wetzel, 1961, p. 339).

PITHONELLA OVALIS (Kaufmann *in* Heer, 1865) new combination

1865 *Lagena ovalis*, KAUFMANN *in* HEER, p. 194–197, figs. 104, 107 (basionym).
1902 *Pithonella ovalis* (Kaufmann *in* Heer 1865); LORENZ, p. 46, pl. 1, fig. 2.
1964 *Pithonella ovalis* (Kaufmann *in* Heer 1865); BIGNOT AND LEZAUD, p. 140, figs. 2, 3, pl. 1, figs. 8–11, pl. 2, figs. 1–10, pl. 3, figs. 1, 2.
1975 *Pithonella ovalis* (Kaufmann *in* Heer 1865); VILLAIN, p. 193–242, pl. 9, figs. 10, 11.
1977 *Pithonella ovalis* (Kaufmann *in* Heer 1865); VILLAIN, p. 146, pl. 1, figs. 2–16, 19, pl. 3, figs. 1, 5–7, 11.
1994 *Pithonella ovalis* (Kaufmann *in* Heer 1865); KEUPP AND KIENEL, p. 199–201.
1994 *Pithonella ovalis* (Kaufmann *in* Heer 1865); ZÜGEL, p. 24–29, pl. 2, figs. 3–8.

Diagnosis.—Ovoid shell with an apical, circular to sub-angular operculum, and with an apical and an antapical pore; apical pole of the ovoid is less convex than the antapical pole; length-width ratio 1.1 to 2.0; a system of dense longitudinal rows of slit-shaped pores spans the double-walled shell; the thin, veneer-like outer wall consists of smooth, shingle-like plates in slightly wavy

→

FIGURE *18*—Additional *Pithonella* species present in the Turonian sediments from Tanzania. *1*, *Pithonella perlonga*, note slit pore rows and outer wall morphology similar to *Pithonella ovalis*; *2, Pithonella trejoi*, etched specimen showing distal surface of inner wall and rows of pores (compare to *12.2*); *3, Pithonella diconica*, holotype, showing partly preserved outer wall (smooth areas) and rows of pores; *4, Pithonella diconica*, etched specimen with opening, and showing "tube-like" slit pore; *5, Pithonella discoidea*, *5a,* large specimen with operculum suture and intermediate diagenetic overgrowth, scale=20 μm; *5b,* enlarged operculum, note spiral pattern in overgrowth reflecting the underlying structure of the outer wall, scale=20 μm; *5c,* detail of apical pore with adjacent area where outer wall with overgrowth are broken off, revealing rod-shaped crystallites on the inner wall surface (compare to *9.4*); *5d,* wall cross-section showing tube-like pores and the typical layered, zigzagging crystallite structure between pores (compare to *6.4*); *6, Pithonella discoidea*, slightly apically shifted position of equatorial bulge, outer wall is not preserved, inner wall surface shows rod-shaped crystallites and rows of pores with denser pore linings and less dense inter-pore areas. All scales=10 μm unless noted otherwise.

https://doi.org/10.1666/12-121 Published online by Cambridge University Press

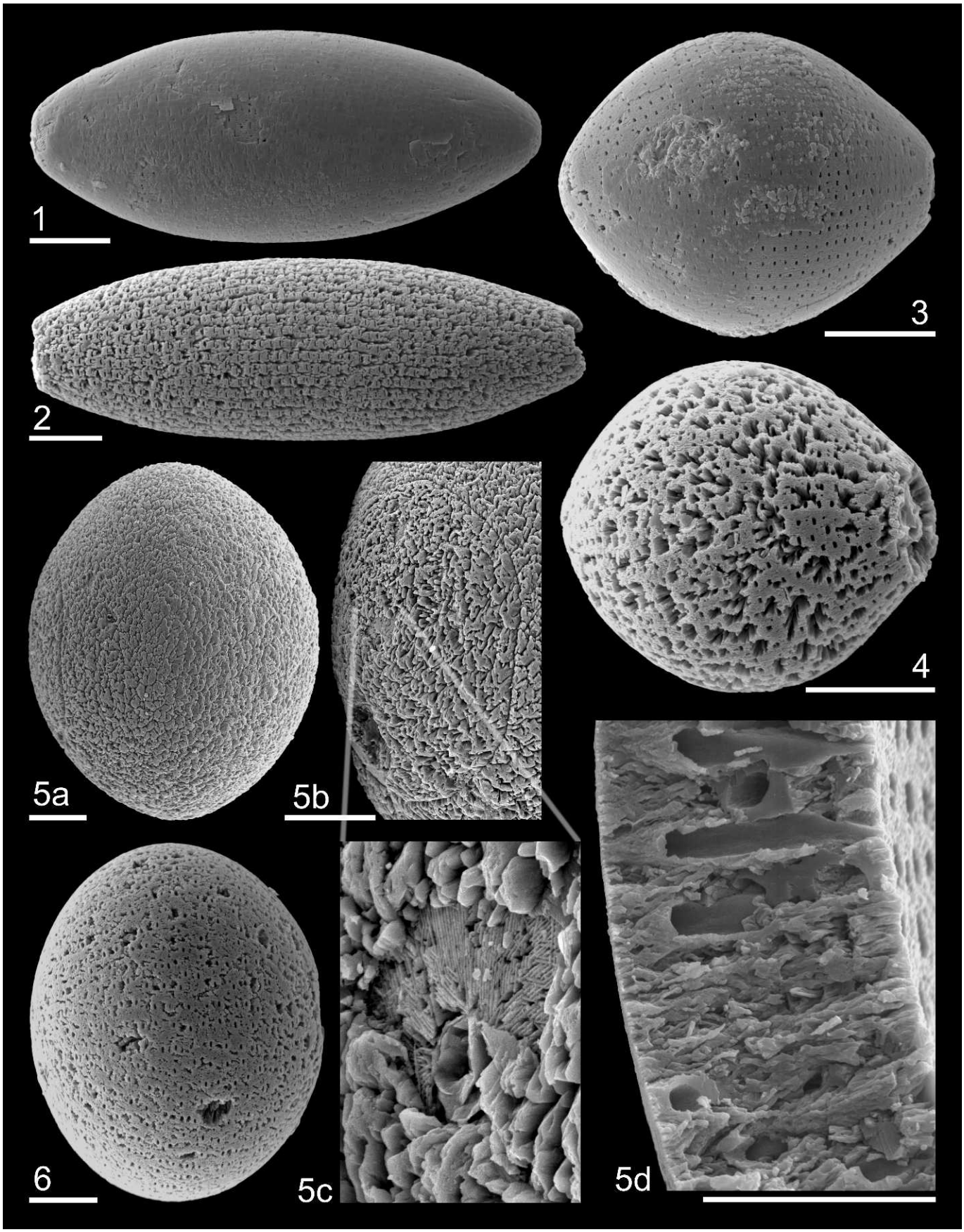

https://doi.org/10.1666/12-121 Published online by Cambridge University Press

longitudinal rows that can spiral at the poles; crypto-crystalline, laminated inner wall with parallel, rod-shaped crystallites on its distal surface; the sub-micron wall-crystallites have a radial, uniformly inclined (pithonellid) crystallographic orientation.

Description.—Given in the Results section of this study. Dimensions: the antapical–apical length is 25–100 μm, the equatorial diameter is 22–90 μm.

Neotype.—Cyst number TDP22-31-1P_E5 sample # TDP22-31-1 (34–45 cm) (Figs. 9.2, 17). The neotype is stored on SEM stub TDP22-31-1P at the National Museum of Natural History, Smithsonian Institution, Washington, D.C., U.S.A. (USNM catalog number 559587).

Material.—Two-hundred thirty-eight (238) specimens from five samples of TDP Site 22.

Occurrence.—Upper Aptian–Cretaceous/Paleogene boundary; Tanzania; Tethyan Realm, between latitudes 40°N and 40°S, global.

Remarks.—The diagnosis has been emended. *Pithonella ovalis* is separated from *P. sphaerica* by the minimum length–width ratio of 1.1, and from *P. multicava* (=*P. perlonga*) by the maximum length–width ratio of 2.0. Early diagenetic recrystallization of surface crystallites to regular parquet-like rows is common and these parquet-like surface patterns represent and additional, secondary, diagnostic trait for the commonly less well-preserved material. According to Zügel (1994), they reflect an anti-clockwise inclination of the surface-crystallites (in apical view).

Pithonella has priority over the original genus assignment by Kaufmann to *Lagena* because *Lagena* is a valid foraminiferal genus. Although *Lagena sphaerica* was also introduced by Kaufmann (1865), Lorenz (1902) described only *Pithonella ovalis* because, using thin sections, he developed the false concept that the circular shapes were merely equatorial cutting planes of *P. ovalis*, making the specimens appear spherical. Because the type material is a thin section showing none of the key traits of *P. ovalis*, and the original material has not been curated, here we provide a neotype from TDP Site 22 as the nomenclatural type both of *Pithonella ovalis* and the genus *Pithonella*.

Pithonella diconica new species
Figure 18.3, 18.4

Diagnosis.—Apically–antapically elongated shell with a pronounced equatorial bulge creating a biconical cyst shape (Fig. 18.3, 18.4); length-width ratio is ~1.25; a system of dense longitudinal rows of slit-shaped pores spans the cell-wall; shell double-walled with an apical, circular to sub-angular operculum, and with an apical and an antapical pore; the sub-micron wall-crystallites have a radial, uniformly inclined (pithonellid) crystallographic orientation.

Description.—Cyst length, 25(33.5)39 μm (nine specimens measured); equatorial diameter, 20(28.1)34 μm. The apical, circular to sub-angular opening is ~6 μm in diameter. The thin, veneer-like outer wall consists of smooth, shingle-like plates in slightly wavy longitudinal rows that can spiral at the poles. The crypto-crystalline, laminated inner wall shows parallel, rod-shaped crystallites on its distal surface.

Etymology.—From *di* (Greek, two), *conos* (Greek, cone) due to the shape resembling two cones connected to each other by their bases.

Types.—Holotype: cyst number TDP22-31-1-P_B4 (44–45cm)=catalog number USNM 547643; paratypes: eight additional specimens: cyst numbers TDP22-22-2_S_B5 (59–76cm)=USNM 547644, TDP22-22-1_I5 (2–20cm)=USNM 547645, TDP22-2_E3 (59–76cm)= USNM 547646, TDP22-2_E8 (59–76cm)= USNM 547647, TDP22-31-1_G4 (44–45cm)= USNM 547648, TDP22-31-1_H4 (44–45cm)= USNM 547649, TDP22-31-1_5a (4–45cm)= USNM 547650, TDP22-36-1_J11 (0–18cm)= USNM 547651. Type specimens are stored on SEM stubs at the National Museum of Natural History, Smithsonian Institution, Washington, D.C., USA.

Occurrence.—Presently observed only in the middle Turonian *Helvetoglobotruncana helvetica* foraminiferal zone of the Nangurukuru Formation in Tanzania, TDP Site 22.

Remarks.—*Pithonella diconica* differs from *P. ovalis* in its outer shape due to distinctive equatorial bulge. The species has a smaller size range.

CONCLUSIONS

An operculum with a distinct suture and crystallographic orientation was discovered in the pithonellid genus *Pithonella*. In its center lies a sub-angular or circular pore. Presence of this operculum indicates that pithonellid calcitarchs represent vegetative or reproductive cysts. The pithonellid opercula have spherical to sub-angular shapes that, together with the central pore, could be interpreted to reflect a plate pattern and corresponding archeopyle types (3A) arising from a peridinoid tabulation. Presence of an operculum and its potential reflection of tabulation support an affinity of the genus *Pithonella* with the dinoflagellates. Alternatively, the documented polygonal shape could simply reflect a penta- or hexa-radial symmetry to be inherent to the pithonellid shell architecture.

Two new aspects have to be included into a revised genus description: 1) The outer wall is ~0.1 μm thin and consists of longitudinally-oriented, parallel rows of shingle-shaped crystallite plates of ~0.8 × 0.8 μm. The basic building units of both the outer and inner walls of *Pithonella* are densely packed crypto-crystalline sub-micron scale (~100 nm) crystals. The crypto-crystalline structure results in a homogeneous appearance of the inner wall in cross-section but it seems to consist of multiple nm-thin concentric individual layers that become visible with slight recrystallization. On the distal surface of the inner wall two layers of parallel, rod-shaped crystallites run in a spiral pattern across the cyst with an angle of ~55° in the orientation of the crystallites between the two layers; and 2) A system of parallel rows of slit-shaped pores is present. In the wall-section these pores are radial, antapically inclined, in-line with the crystallographic orientation.

The Tanzanian material provides a rare preservation window with exquisitely preserved specimens. The reported new microstructures are unlike any that have been previously described as these are rapidly obliterated with recrystallization. Importantly, our detailed observations of the wall architecture and crystallography of *Pithonella* support existing models of pithonellid biomineralization that have been associated with biomineralization features of the Thoracosphaeraceae. Taxonomic accuracy has been limited until now because *Pithonella* has been described only from less well-preserved material. A regular parquet-pattern in straight or spiraling rows of prismatic crystals, as emphasized in previous *Pithonella* descriptions, is here determined to be a diagenetic artifact.

The wall chemistry of *Pithonella* cysts reveals calcite characterized by a relatively high Mg content. Comparison of $\delta^{18}O$ values from *Pithonella* and co-occurring benthic and planktonic foraminifera indicate the cysts grew in surface waters. A relatively enriched $\delta^{13}C$ value may be related to photosynthetic activity but differs from known values of calcareous dinoflagellates, suggesting inter-specific differences in vital effects.

Although cysts of several organisms other than dinoflagellates require an operculum in order to facilitate hatching, an affiliation of *Pithonella* with these groups is considered unlikely

because of differences in habitat, crystallographic orientation, and mineralogical composition. On the other hand, an exclusive affiliation of the genus *Pithonella* with calcareous dinoflagellates remains debatable even with superb preservation, due to the absence of unequivocal, complete dinoflagellate tabulation.

ACKNOWLEDGMENTS

This research was funded by the German Science Foundation (grant WE 4587/1-1), National Science Foundation (NSF EAR 0641956) and the Smithsonian Institution's Charles Walcott Fund and Scholarly Studies Program. We thank the Tanzania Petroleum Development Corporation, and particularly Dr. J. Singano, for logistical support and the Tanzania Commission for Science and Technology for permission to drill. J. Wingerath, S. Whittaker, A. Logan, T. Rose (Smithsonian Institution) are acknowledged for technical assistance. K.G. MacLeod (University of Missouri) performed stable isotope measurements. M. Kirsch provided culture material and gave perspectives and comparisons with recent dinoflagellates. We acknowledge inspiring discussions with H. Keupp, G. Versteegh, and H. Willems. We thank S. Meier, M. Streng and M. Head for insightful reviews and fruitful communication that strongly improved the manuscript.

REFERENCES

ANDRI, E. 1972. Mise au point et données novelles sur la famille des Calcisphaerulidae Bonet 1956: Les genres *Bonetocardiella*, *Pithonella*, *Calcisphaerula* et *Stomiosphaera*. Revue de Micropaléontologie, 15:12–34.

BEIN, A. AND Z. REISS. 1976. Cretaceous *Pithonella* from Israel. Micropaleontology, 22:83–91.

BIGNOT, G. AND L. LEZAUD. 1964. Contribution à l'étude des *Pithonella* de la Craie Parisienne. Revue de Micropaléontologie, 7:138–152.

BOLLI, H. M. 1974. Jurassic and Cretaceous Calcisphaerulidae from DSDP leg 27, Eastern Indian Ocean. Initial Reports of the Deep Sea Drilling Project, 27:843–907.

BONET, F. 1956. Zonificación microfaunística de las calizas cretácicas del este de México. Boletin de la Asociación Mexicana de Geólogos Petroleros, 8: 389–488.

BORZA, K. 1972. Neue Arten der Gattungen *Cadosina* Wanner, *Pithonella* Lorenz und *Palinosphaera* Reinsch aus der oberen Kreide. Geologica Carpathica, 23:139–150.

BÜTSCHLI, O. 1885. Dinoflagellata. Dr. H. G. Bronn's Klassen und Ordnungen des Thier-Reichs, wissenschaftlich dargestellt inWort und Bild. II. Abtheilung: Mastigophora. C. F. Winter'sche Verlagshandlung, Leipzig und Heidelberg, p. 906–1029.

COLOM, G. 1955. Jurassic–Cretaceous pelagic sediments of the western Mediterranean zone and the Atlantic area. Micropaleontology, 1:109–124.

DALI-RESSOT, M.-D. 1987. Les Calcisphaerulidae des terrains Albien a Maastrichtien de Tunisie centrale (J. Bireno et J. Bou el Ahneche): Intérêt systématique, stratigraphique et paléogéographique. Unpublished Ph.D. dissertation, University of Tunis, Tunis, 191 p.

DEFLANDRE, G. 1947. *Calciodinellum* nov. gen., premier représentant d'une famille nouvelle de dinoflagellés à thèque calcaire. Comptes rendus hebdomadaires des séances de l'Académie des sciences, 224:1781–1782.

DIAS-BRITO, D. 2000. Global stratigraphy, palaeobiogeography and palaeoecology of Albian–Maastrichtian pithonellid calcispheres: Impact on Tethys configuration. Cretaceous Research, 21:315–349.

DUFOUR, T. 1968. Quelques remarques sur les organismes Incertae sedis de la famille des Calcisphaerulidae Bonet 1956. Compte rendu hebdomadaire des séances de l'Académie des sciences, Série D, 266:1947–1949.

EHRENBERG, C. G. 1831. Animalia evertebrata, p. [unpaginated]. *In* P. C. Hemprich and C. G. Ehrenberg (eds.), Symbolae physicae seu icones et descriptiones naturalium novorum aut minus cognitorum quae ex itineribus Lybiam Aegyptum Nubiam Dongalam Syriam Arabiam et Habessinian. Pars Zoologica. Abhandlungen der deutschen Akademie der Wissenschaften.

ELBRÄCHTER, M., M. GOTTSCHLING, T. HILDEBRAND-HABEL, H. KEUPP, R. KOHRING, J. LEWIS, K. J. S. MEIER, M. MONTRESOR, M. STRENG, G. J. M. VERSTEEGH, H. WILLEMS, AND K. ZONNEVELD. 2008. Establishing an Agenda for Calcareous Dinoflagellate Research (Thoracosphaeraceae, Dinophyceae) including a nomenclatural synopsis of generic names. Taxon, 57: 1289–1303.

EVITT, W. R. 1967. Dinoflagellate studies II. The archeopyle. Stansford University Publications Geological Sciences, 10(3):1–83.

EVITT, W. R. 1985. Sporopollenin dinoflagellate cysts: Their morphology and interpretation. AASP Monograph Series, 1:1–333.

FARZADI, P. 2006. The development of middle Cretaceous carbonate platforms, Persian Gulf, Iran: Constraints from seismic stratigraphiy, well and biostratigraphy. Petroleum Geoscience, 12:59–68.

FENSOME, R. A., F. J. R. TAYLOR, G. NORRIS, W. A. S. SARJEANT, D. I. WHARTON, AND G. L. WILLIAMS. 1993. A classification of living and fossil dinoflagellates. Micropaleontology Special Publication 7, 351 p.

FRIEDRICH, O. AND K. J. S. MEIER. 2003. Stable isotopic indication for the cyst formation depth of Campanian/Maastrichtian calcareous dinoflagellates. Micropaleontology, 49:375–380.

FRIEDRICH, O. AND K. J. S. MEIER. 2006. Suitability of stable oxygen and carbon isotopes of calcareous dinoflagellate cysts for paleoclimatic studies: Evidence from the Campanian/Maastrichtian cooling phase. Palaeogeography, Palaeoclimatology, Palaeoecology, 239:456–469.

FÜTTERER, D. K. 1977. Distribution of calcareous dinoflagellates in Cenozoic sediments of Site 366, Eastern North Atlantic. Initial Reports of the Deep Sea Drilling Project, 41:709–737.

FÜTTERER, D. K. 1984. Pithonelloid calcareous dinoflagellates from the upper Cretaceous and cenozoic of the southeastern Atlantic Ocean, deep Sea Drilling Project Leg–74. Initial Reports of the Deep Sea Drilling Project, 74:533–541.

GAO, X., J. D. DODGE, AND J. LEWIS. 1989. An ultrastructural study of planozygotes and encystment of a marine dinoflagellate, *Scrippsiella* sp. British Phycological Journal, 24:153–165.

HAECKEL, E. 1894. Systematische Phylogenie. Entwurf eines natürlichen Systems der Organismen auf Grund ihrer Stammesgeschichte, I. Systematische Phylogenie der Protisten und Pflanzen. Reimer, Berlin, 400 p.

HO, T.-Y., A. QUIGG, Z. V. FINKEL, A. J. MILLIGAN, K. WYMAN, P. G. FALKOWSKI, AND F. M. M. MOREL. 2003. The elemental composition of marine phytoplankton. Journal of Phycology, 39:1145–1159.

HÖLL, C., K. A. F. ZONNEVELD, AND H. WILLEMS. 1998. On the ecology of calcareous dinoflagellates: The quaternary eastern Equatorial Atlantic. Marine Micropaleontology, 33:1–25.

HUBER, B. T. AND M. R. PETRIZZO. In Press. Evolution and taxonomic study of the Cretaceous planktonic foraminifer genus Helvetoglobotruncana Reiss, 1957. Journal of Foraminiferal Research, 44.

JANOFSKE, D. 1992. Kalkiges Nannoplankton, insbesondere kalkige Dinoflagellaten-Zysten der alpinen Ober-Trias: Taxonomie, Biostratigraphie und Bedeutung für die Phylogenie der Peridiniales. Berliner Geowissenschaftliche Abhandlungen Reihe E, 4:1–53.

JANOFSKE, D. 1996. Ultrastructure types in recent calcispheres. Bulletin de l'Institut océanographique, 14:295–303.

JANOFSKE, D. AND B. KARWATH. 2000. Oceanic calcareous dinoflagellates of the equatorial Atlantic Ocean: Cyst-theca relationship, taxonomy and aspects on ecology, p. 93–136. *In* B. Karwath (ed.), Ecological Studies on Living and Fossil Calcareous Dinoflagellates of the Equatorial and Tropical Atlantic Ocean. Volume 152. Bremen University Berichte, Bremen.

JIMÉNEZ BERROCOSO, Á., B. T. HUBER, K. G. MACLEOD, M. R. PETRIZZO, J. A. LEES, I. WENDLER, H. COXALL, A. K. MWENEINDA, F. FALZONI, H. BIRCH, J. M. SINGANO, S. HAYNES, L. COTTON, J. WENDLER, P. R. BOWN, S. ROBINSON, AND J. GOULD. 2012. Lithostratigraphy, biostratigraphy and chemostratigraphy of upper Cretaceous and Paleocene sediments from southern Tanzania: Tanzania Drilling Project Sites 27–35. Journal of African Earth Sciences, 70:36–57.

JIMÉNEZ BERROCOSO, Á., K. G. MACLEOD, B. T. HUBER, J. A. LEES, I. WENDLER, P. R. BOWN, A. K. MWENEINDA, C. ISAZA LONDOÑO, and J. M. Singano. 2010. Lithostratigraphy, biostratigraphy and chemostratigraphy of upper Cretaceous sediments from southern Tanzania: Tanzania Drilling Project Sites 21 to 26. Journal of African Earth Sciences, 57:47–69.

KAUFMANN, F. J. 1865. Polythalamien des Seewerkalkes, p. 194–199. *In* O. Heer (ed.), Die Urwelt der Schweiz, Zuerich.

KERNTOPF, B. 1997. Dinoflagellate distribution patterns and preservation in the equatorial Atlantic and offshore North-West Africa. Berichte Fachbereich Geowissenschaften Bremen, 103:1–137.

KEUPP, H. 1981. Calcareous dinoflagellate-cysts of the boreal lower Cretaceous (lower Hauterivian to lower Albian. Facies, 5:1–190.

KEUPP, H. 1987. Die kalkigen Dinoflagellatenzysten des Mittelalb bis Untercenoman von Escalles/Boulonnais (N-Frankreich). Facies, 16:6–21.

KEUPP, H. 1990. A new pithonelloid calcareous dinoflagellate cyst from the upper Cretaceous of South Dakota/U.S.A. Facies, 22:47–58.

KEUPP, H. AND U. KIENEL. 1994. Wandstrukturen bei Pithonelloideae (Kalkige Dinoflagellaten-Zysten): Biomineralisation und systematische Konsequenzen. Abhandlungen der Geologischen Bundesanstalt, 50:197–217.

KEUPP, H., B. MONNET, AND R. KOHRING. 1991. Morphotaxa bei kalkigen Dinoflagellaten-Zysten und ihre problematische Systematisierung. Berliner geowissenschaftliche Abhandlungen A, 134:161–185.

KIENEL, U. 1994. Die Entwicklung der kalkigen Nannofossilien und der kalkigen Dinoflagellaten-Zysten an der Kreide/Tertiär-Grenze in Westbrandenburg im Vergleich mit Profilen in Nordjütland und Seeland (Dänemark). Berliner Geowissenschaftliche Abhandlungen Reihe E, 12:88.

KOHN, M. AND K. A. F. ZONNEVELD. 2010. Calcification depth and spatial distribution of *Thoracosphara heimii*; implications for palaeoceanographic reconstructions. Deep-Sea Research I, 57:1543–1560.

KOHRING, R., M. GOTTSCHLING, AND H. KEUPP. 2005. Examples for character traits and palaeoecological significance of calcareous dinoflagellates. Paläontologische Zeitschrift, 79:79–91.

LOCKER, S. 1967. Die Sphaeren der Oberkreide und die sogenannte Orbulinaritfazies. Geologie, 16:850–859.

LORENZ, T. 1902. Geologische Studien im Grenzbereich zwischen helvetischer und ostalpiner Fazies. II. Teil: Südlicher Rhaetikon. Berichte der naturforschenden Gesellschaft Freiburg i. Br., 12:34–62.

MACLEOD, K. G., B. T. HUBER, Á. JIMÉNEZ BERROCOSO, AND I. WENDLER. In press. A stable, hot and ice-free Cretaceous greenhouse based on Turonian samples from Tanzania. Geology.

MARSZALEK, D. S. 1975. Calcisphere ultrastructure and skeletal aragonite from the algae *Acetabularia antillana*. Journal of Sedimentary Petrology, 45: 266–271.

MASTERS, B. A. AND R. W. SCOTT. 1978. Microstructure, affinities and systematics of Cretaceous calcispheres. Micropaleontology, 24:210–221.

MEIER, K. J. S., N. ENGEMANN, M. GOTTSCHLING, AND R. KOHRING. 2009. Die Bedeutung der Struktur der Zystenwand kalkiger Dinoflagellaten (Thoracosphaeraceae, Dinophyceae). Berliner palaeobiologische Abhandlungen, 10:245–256.

NORRIS, R. D. 1998. Recognition and macroevolutionary significance of photosymbiosis in molluscs, corals, and foraminifera. The Paleontological Society Papers, 4:68–100.

ODIN, G. S. 2011. Gilianelles: Late Cretaceous microproblematica from Europe and Central America. Palaeontology, 54:133–144.

PASCHER, A. 1914. Über Flagellaten und Algen. Berichte der Deutschen Botanischen Gesellschaft Berlin, 32:136–160.

PIRYAEU, A., J. J. G. REIJMER, F. S. P. VAN BUCHEM, M. YAZDI-MOGHADAM, J. SADOUNI, AND T. DANELIAN. 2011. The influence of Late Cretaceous tectonic processes on sedimentation patterns along the northeastern Arabian plate margin (Fars Province, SW Iran). Journal of the Geological Society, Special Publications, 168:235–250.

SCHILLER, J. 1930. Coccolithineae, p. 89–267. *In* L. Rabenhorst (ed.), Kryptogamen Flora von Deutschland, Osterreich und der Schweiz. Volume 10. Akademische Verlagsgesellschaft, Leipzig.

SOLMS-LAUBACH, H. 1895. Monograph of the Acetabularieae. Transactions of the Linnean Society, 5:1–39.

STRENG, M., T. HILDEBRAND-HABEL, AND H. WILLEMS. 2004. A proposed classification of archeopyle types in calcareous dinoflagellate cysts. Journal of Paleontology, 78:456–483.

VERSTEEGH, G. J. M. 1993. New Pliocene and Pleistocene calcareous dinoflagellate cysts from southern Italy and Crete. Review of Palaeobotany and Palynology, 78:353–380.

VERSTEEGH, G. J. M., T. SERVAIS, M. STRENG, A. MUNNECKE, AND D. VACHARD. 2009. A discussion and proposal concerning the use of the term calcispheres. Palaeontology, 52:343–348.

VILLAIN, J.-M. 1975. "Calcispherulidae" (incertae sedis) du Cretacé supérieur du Limbourg (Pays-Bas), et d'autre régions. Palaeontographica Abt. A, 149: 193–242.

VILLAIN, J.-M. 1977. Les Calcisphaerulidae: Architectures, calcification de la paroi et phylogenèse. Paleontographica Apt. A, 159:139–177.

VILLAIN, J.-M. 1981. Les Calcisphaerulidae: Intérêt stratigraphique et paléoécologique. Cretaceous Research, 2:435–438.

VILLAIN, J.-M. 1992. Calciphaerulidae d'Afrique: Les stades juvéniles de *Pithonella* Lorenz, 1902, structure et minéralisation des tests Geologie Africaine: Coll. Geol. Libreville, recueil des communication, 6–8, May 1991, p. 339–245.

VOGLER, J. 1941. Oberer Jura von Misel (Niederländisch–Ostindien). Paleontographica, 4:245–293.

VOIGT, E. AND W. HÄNTZSCHEL. 1964. Gradierte Schichtung in der Oberkreide Westfalens. Fortschritte in der Geologie von Rheinland und Westfalen, 7: 495–548.

WEFER, G. 1985. Die Verteilung stabiler Isotope in Kalkschalen mariner Organismen. Geologisches Jahrbuch Reihe A, 82:3–111.

WEINER, S. AND L. ADDADI. 2011. Crystallization pathways in biomineralization. Annual Review of Materials Research, 41:21–40.

WENDLER, I., B. T. HUBER, K. G. MACLEOD, AND J. E. WENDLER. 2011. Early evolutionary history of *Tubulogenerina* and *Colomia*, with new species from the Turonian of East Africa. Journal of Foraminiferal Research, 41: 384–400.

WENDLER, I., B. T. HUBER, K. G. MACLEOD, AND J. E. WENDLER. 2013. Stable oxygen and carbon isotope systematics of exquisitly preserved Turonian foraminifera from Tanzania—understanding isotope signatures in fossils. Marine Micropaleontology, 102:1–33.

WENDLER, J. E., K. U. GRÄFE, AND H. WILLEMS. 2002a. Palaeoecology of calcareous dinoflagellate cysts in the mid-Cenomanian Boreal Realm: Implications for the reconstruction of palaeoceanography of the NW European shelf sea. Cretaceous Research, 23:213–229.

WENDLER, J. E., K. U. GRÄFE, AND H. WILLEMS. 2002b. Reconstruction of mid-Cenomanian orbitally forced palaeoenvironmental changes based on calcareous dinoflagellate cysts. Palaeogeography, Palaeoclimatology, Palaeoecology, 179:19–41.

WENDLER, J. E., I. WENDLER, B. T. HUBER, AND T. ROSE. 2012. Using cathodoluminescence spectroscopy of Cretaceous calcareous microfossils to distinguish biogenic from early-diagenetic calcite. Microscopy and Microanalysis, 18(6):1–9.

WENDLER, J. E., I. WENDLER, AND H. WILLEMS. 2001. *Orthopithonella collaris* sp. nov., a new calcareous dinoflagellate cyst from the K/T boundary (Fish Clay, Stevns Klint/Denmark). Review of Palaeobotany and Palynology, 115:69–77.

WENDLER, J. E. AND H. WILLEMS. 2002. Distribution pattern of calcareous dinoflagellate cysts across the Cretaceous–Tertiary boundary (Fish Clay, Stevns Klint, Denmark); implications for our understanding of species-selective extinction, p. 265–275. *In* C. Koeberl and K. G. MacLeod (eds.), Catastrophic Events and Mass Extinctions: Impacts and Beyond. Geological Society of America Special Paper 356.

WENDLER, J. E. AND H. WILLEMS. 2004. Pithonelloid wall-type of the Late Cretaceous calcareous dinoflagellate cyst genus *Tetratropis*. Review of Palaeobotany and Palynology, 129(3):133–140.

WENDLER, J. E. AND P. BOWN. 2013. Exceptionally well-preserved Cretaceous microfossils reveal new biomineralization styles. Nature Communications, 4:2052, doi:10.1038/ncomms3052.

WETZEL, O. 1961. New microfossils from Baltic Cretaceous flintstones. Micropaleontology, 7:337–350.

WILLEMS, H. 1990. *Tetratropis*, eine neue Kalkdinoflagellaten-Gattung (Pithonelloideae) aus der Oberkreide von Lägerdorf (N-deutschland). Senckenbergiana lethaea, 70:239–257.

WILLEMS, H. 1992. Kalk-Dinoflagellaten aus dem Uner-Maastricht der Insel Rügen. Zeitschrift der Deutschen Geologischen Wissenschaften, 20:155–178.

WILLEMS, H. 1994. New calcareous dinoflagellates from the upper Cretaceous White Chalk of northern Germany. Review of Palaeobotany and Palynology, 84:57–72.

YOUNG, J. R., J. A. BERGEN, P. R. BOWN, J. A. BURNETT, A. FIORENTINO, R. W. JORDAN, A. KLEIJNE, B. E. VAN NIEL, A. J. T. ROMEIN, AND K. VON SALIS. 1997. Guidelines for coccolith and calcareous nannofossil terminology. Palaeontology, 40:875–912.

ZIVERI, P., H. STOLL, I. PROBERT, C. KLAAS, M. GEISEN, G. GANSSEN, AND J. YOUNG. 2003. Stable isotope 'vital effects' in coccolith calcite. Earth and Planetary Science Letters, 210:137–149.

ZONNEVELD, K. A. F. 2004. Potential use of stable oxygen isotope composition of *Thoracosphaera heimii* (Dinophyceae) for upper watercolumn (thermocline) temperature reconstruction. Marine Micropaleontology, 50:307–317.

ZONNEVELD, K. A. F., A. MACKENSEN, AND K.-H. BAUMANN. 2007. Stable oxygen isotopes of *Thoracosphaera heimii* (Dinophyceae) in relationship to temperature; a culture experiment. Marine Micropaleontology, 64:80–90.

ZÜGEL, P. 1994. Verbreitung kalkiger Dinoflagellaten-Zysten im Cenoman/Turon von Westfrankreich und Norddeutschland. Courier Forschungsinstitut Senckenberg, 176:1–159.

ACCEPTED 16 JUNE 2013